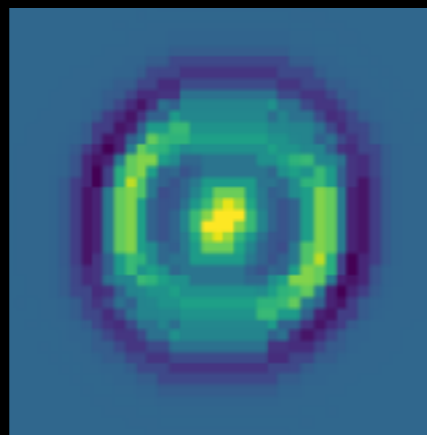
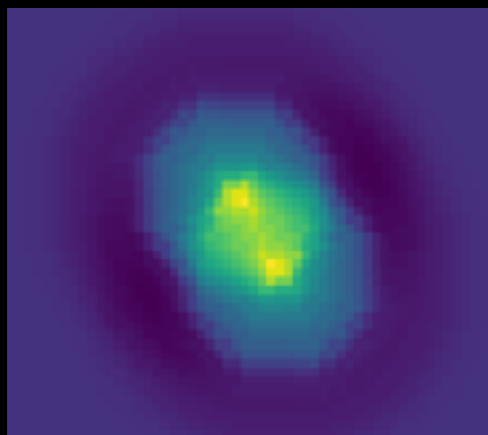


# Cosmological Particle Production & Pairwise Spots on the CMB

Yuhsin Tsai  
University of Notre Dame



Cosmology from Home 2023

Based on **2107.09061** (JHEP 11 (2021) 158) with



Jeong Han Kim  
(Chungbuk National University)



Soubhik Kumar  
(LBNL)



Adam Martin  
(Notre Dame)

And **2303.08869**  
with better signal calculation +  
+ neutral Network analysis



Taegyun Kim  
(Notre Dame)

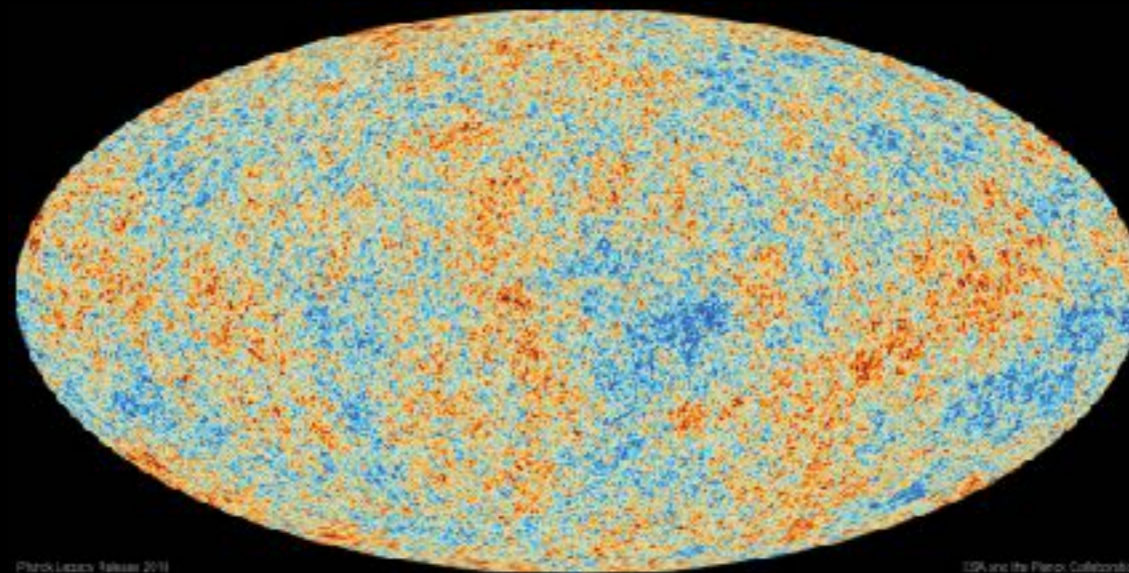


Moritz Munchmeyer  
(UW Madison)

Our goal: probing **extremely heavy particles**  
using **inflationary dynamics + CMB signals**

Our goal: probing **extremely heavy particles**  
using **inflationary dynamics + CMB signals**

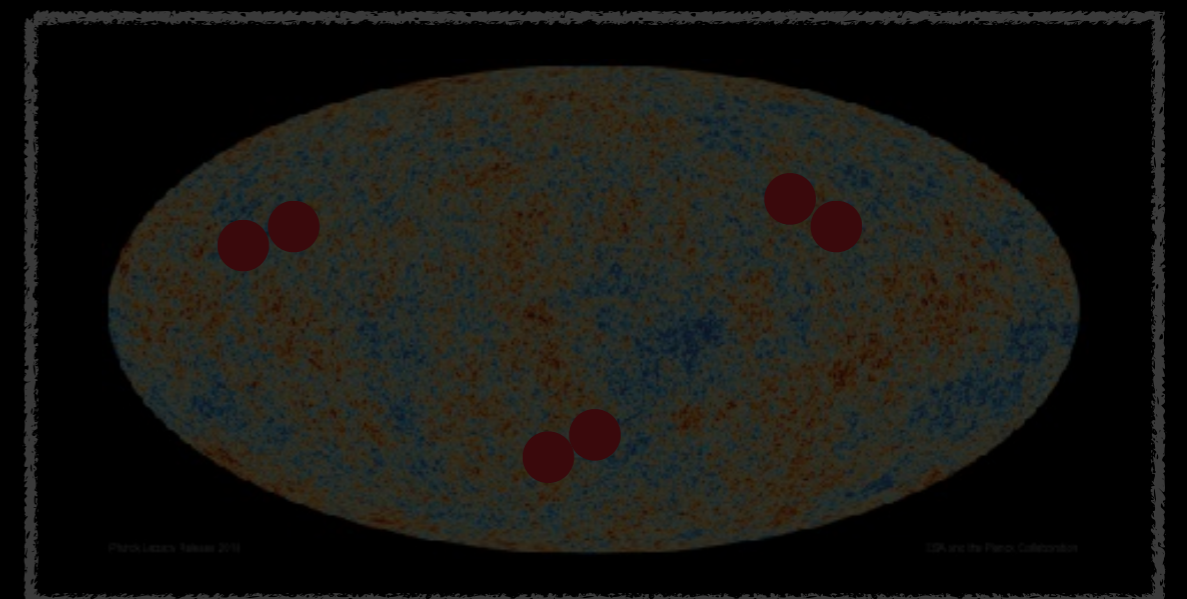
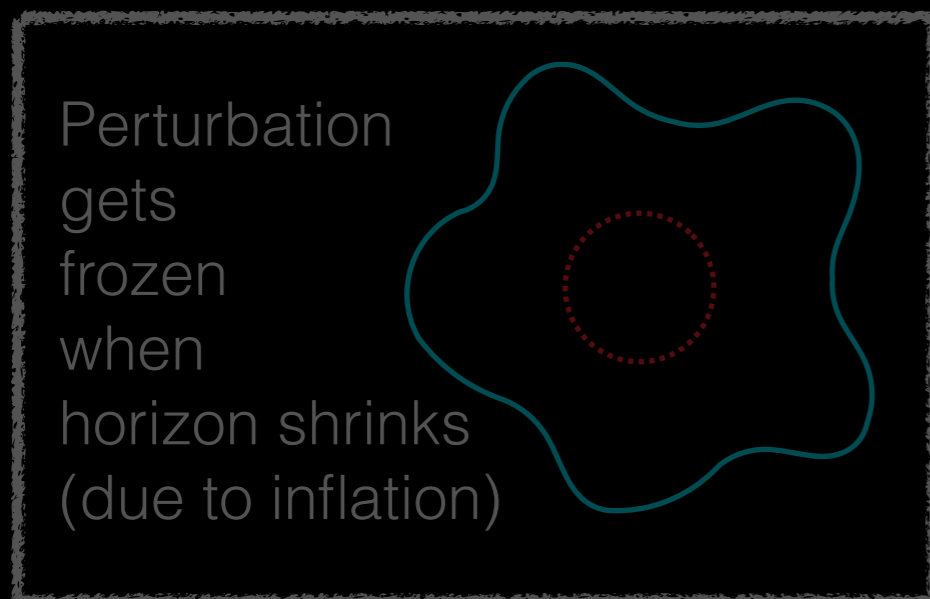
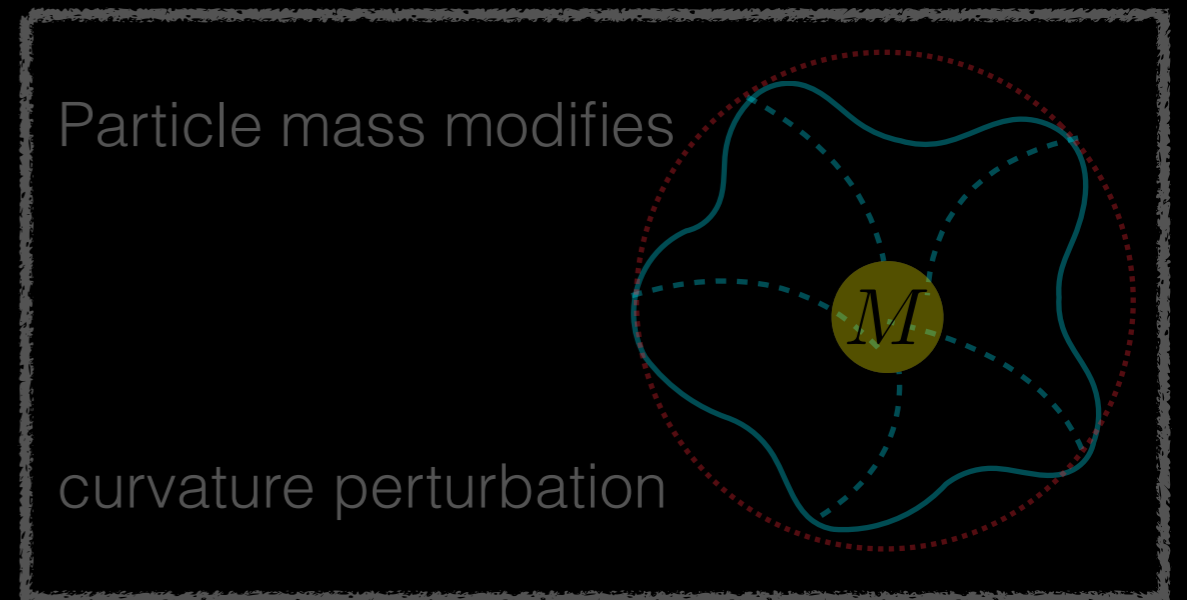
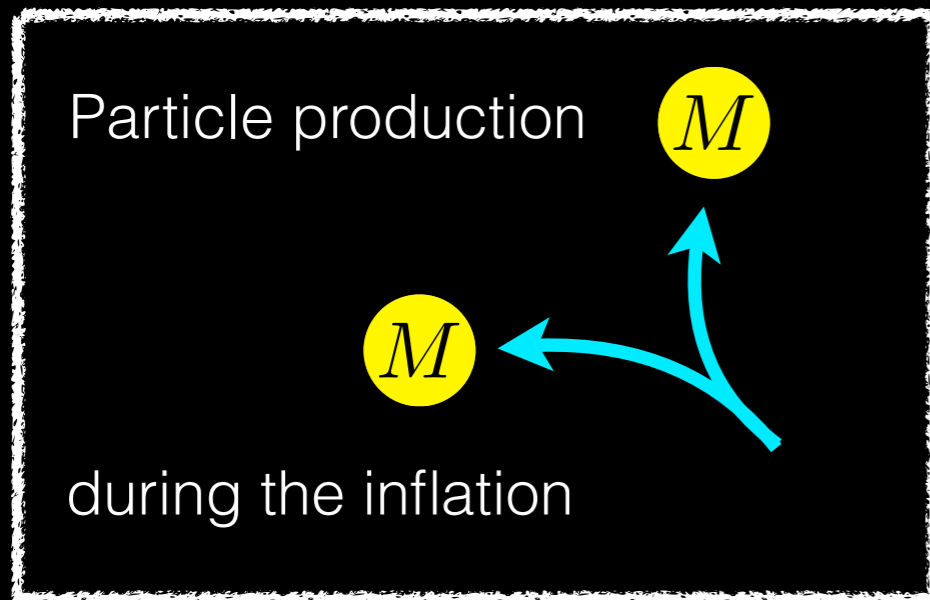
Our **particle detector**: CMB



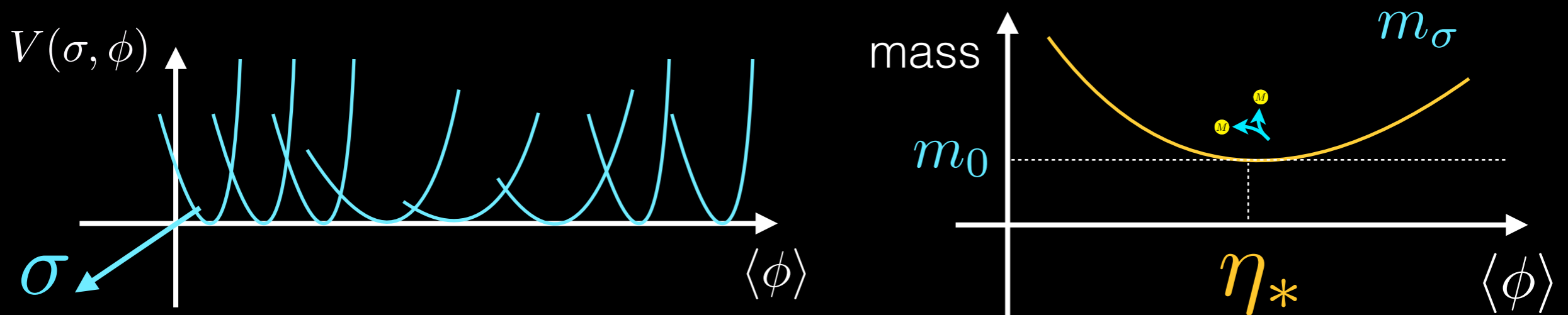
Planck Legacy Release 2018

ESA and the Planck Collaboration

# Step I : the non-adiabatic particle production



Consider a scalar particle  $\sigma$  that carries a mass depending on the inflaton-VEV



- Sigma mass is typically heavy (comparing to Hubble scale)
- mass takes its minimum value at time  $\eta_*$

# Consider inflation-dependent masses in general

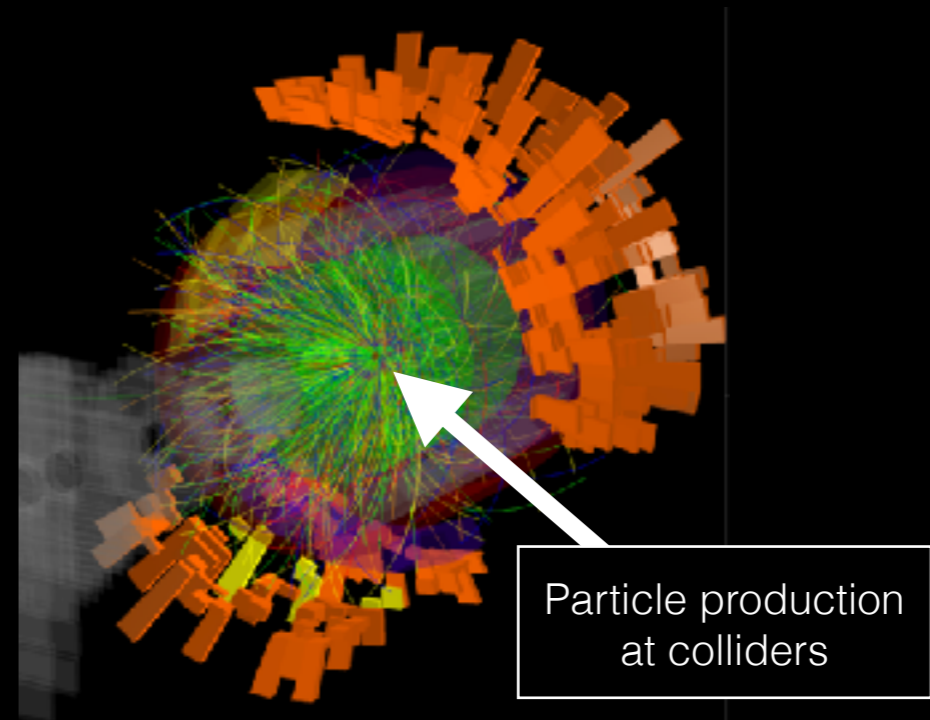
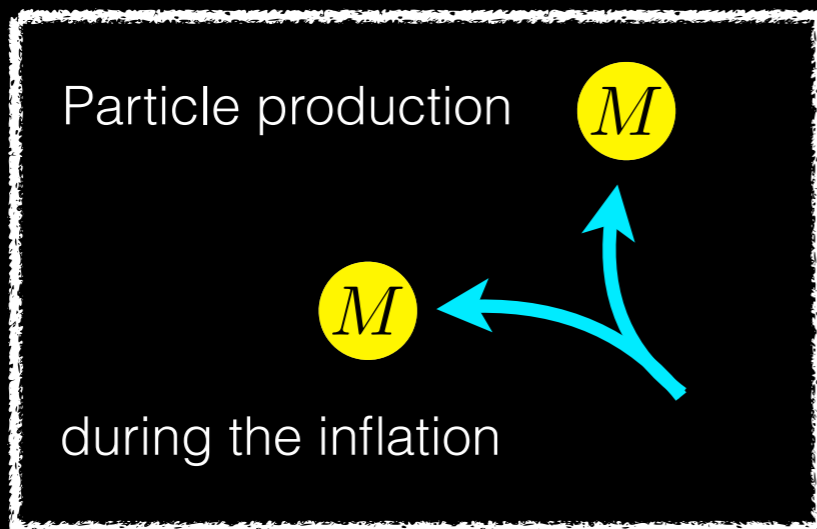
Since particle production only happens around  $\eta_*$   
can re-parametrize the mass without loss of generality

$$\mathcal{L}_\sigma = -\frac{1}{2}(\partial_\mu\sigma)^2 - \frac{1}{2}[(g\phi - \mu)^2 + M_0^2]\sigma^2$$

(also see a similar setup in Flauger et al. (2017),  
and Munchmeyer et al. (2019) for the N-point function study)

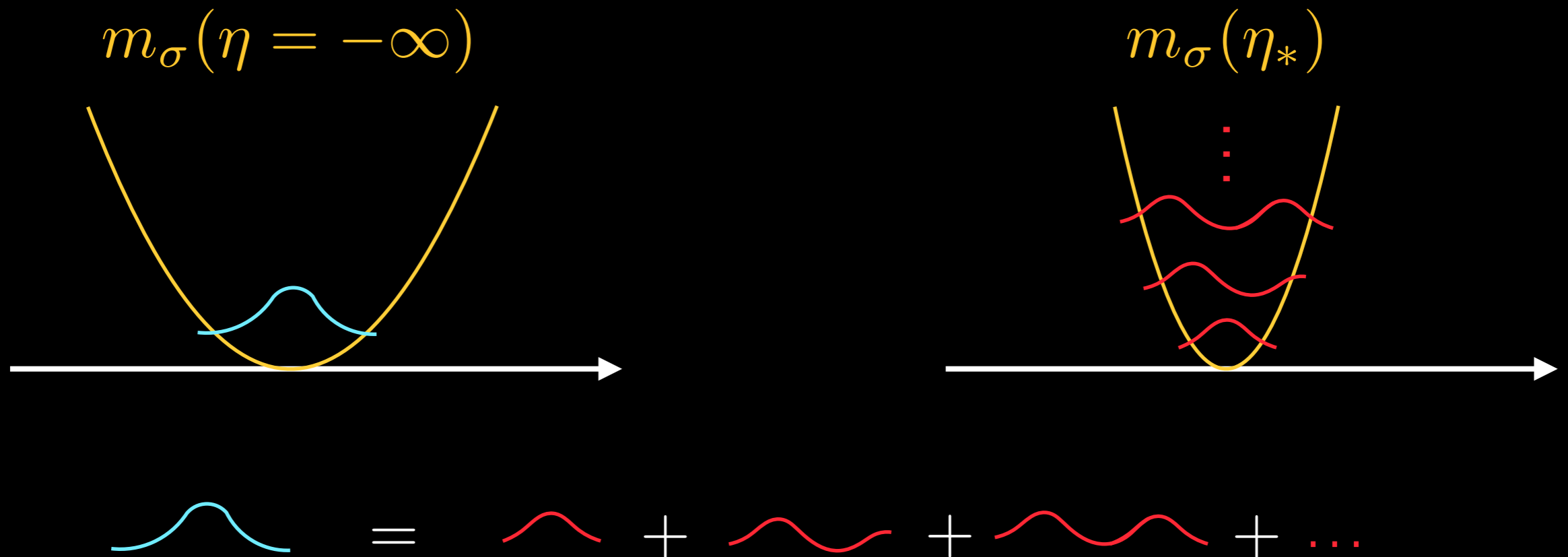
# How to calculate the particle production?

- cannot calculate the production as in collider experiments.  
inflaton & sigma are time-dependent fields & the vacuum changes
- calculate the number of non-adiabatic particle production from **Bogolyubov transformation**





# Particle production from time-variant vacuum



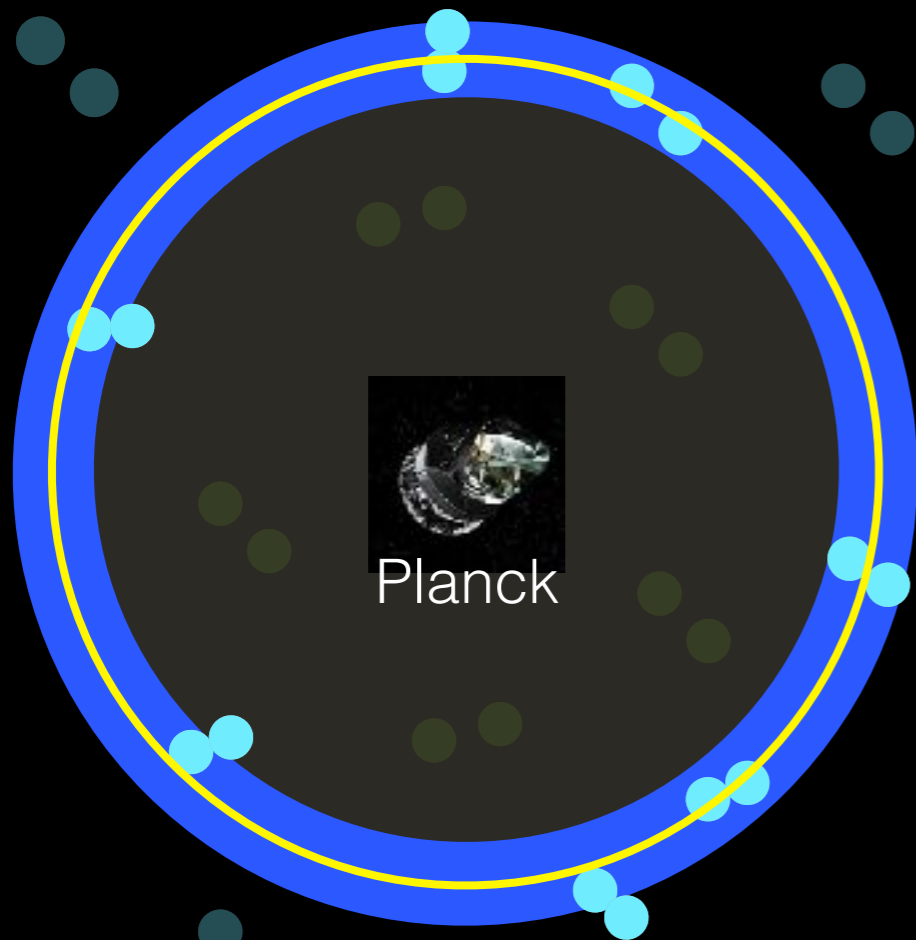
when promoting field into an operator, the initial raising and lowering operators will be a combination of later time raising/lowering operators

$$\begin{aligned} \hat{u}(\eta, \mathbf{x}) &= \int \frac{d^3\mathbf{k}}{(2\pi)^{3/2}} \left[ \hat{a}_{\mathbf{k}} \mathcal{I}_{\mathbf{k}}(\eta) e^{i\mathbf{k}\cdot\mathbf{x}} + \hat{a}_{\mathbf{k}}^\dagger \mathcal{I}_{\mathbf{k}}^*(\eta) e^{-i\mathbf{k}\cdot\mathbf{x}} \right] \\ &= \int \frac{d^3\mathbf{k}}{(2\pi)^{3/2}} \left[ \hat{b}_{\mathbf{k}} \mathcal{F}_{\mathbf{k}}(\eta) e^{i\mathbf{k}\cdot\mathbf{x}} + \hat{b}_{\mathbf{k}}^\dagger \mathcal{F}_{\mathbf{k}}^*(\eta) e^{-i\mathbf{k}\cdot\mathbf{x}} \right] \end{aligned}$$

$\mathcal{I}, \mathcal{F}$  are the initial & final mode functions

# Number of $\sigma$ pairs around the CMB last scattering surface (with $\eta = \eta_{\text{rec}} \pm \eta_*$ )

$$N_{\sigma \text{ pairs}} = \frac{1}{2\pi^2} \left( \frac{g\dot{\phi}_0}{H_I^2} \right)^{3/2} e^{-\frac{\pi(M_0^2 - 2H_I^2)}{g|\dot{\phi}|}} \left( \frac{\eta_0}{\eta_*} \right)^3 \frac{\Delta\eta}{\eta_0}$$



$$M_{\text{eff}}^2 \approx M_0^2 + g^2 \phi'^2 (\eta - \eta_*)^2$$

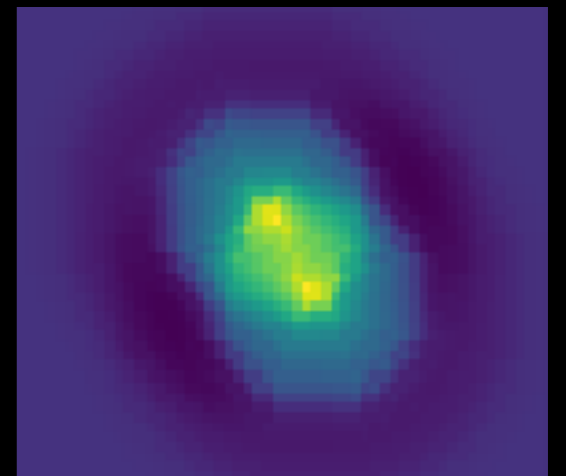
If  $g = 2, M_0 = 200 H_I = 3.3\sqrt{\dot{\phi}}$   
and  $\eta_* = 100 \text{ Mpc}$

(similar to chopping the sky into  $\sim 500 \times 500$  pieces)

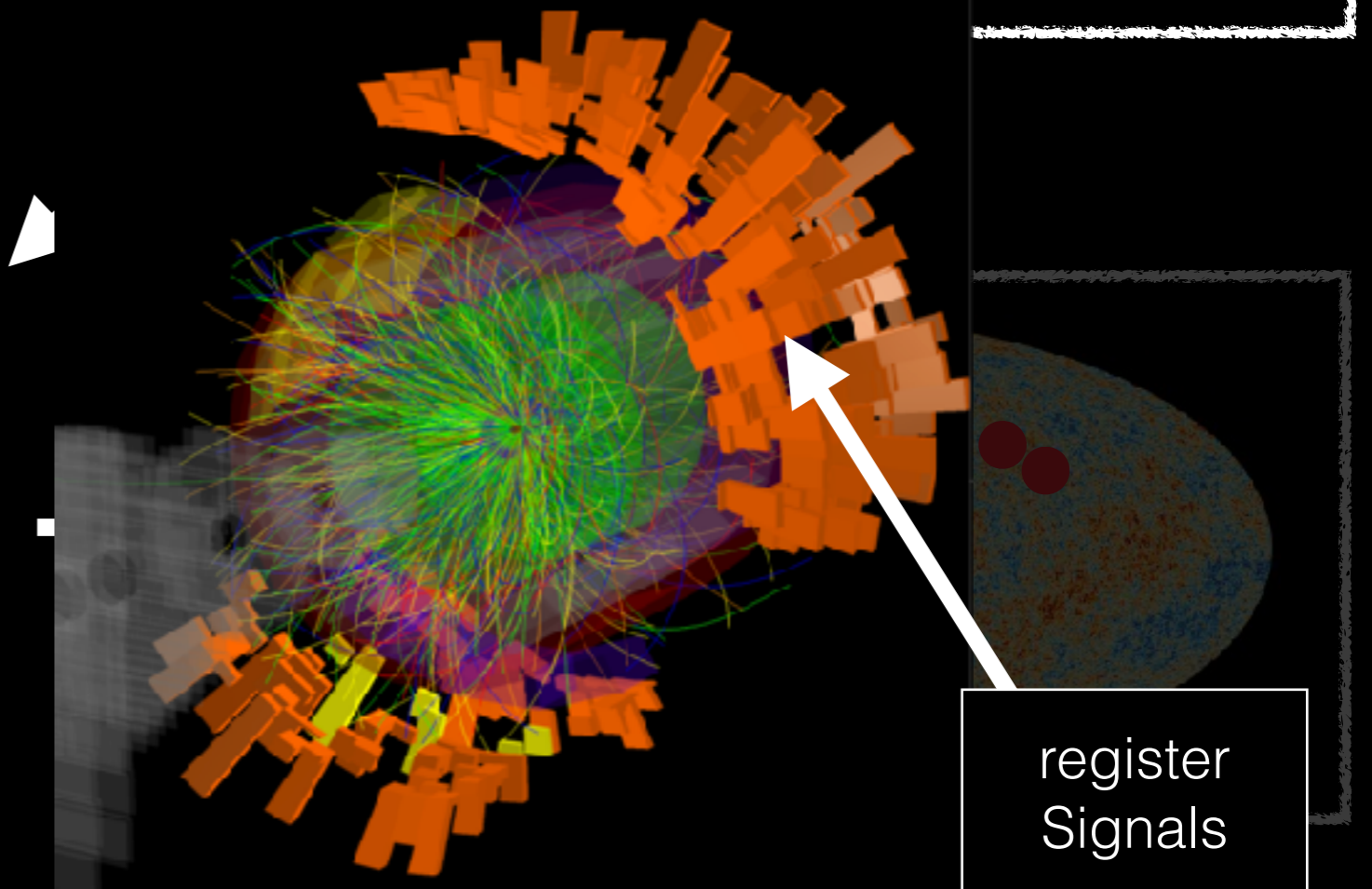
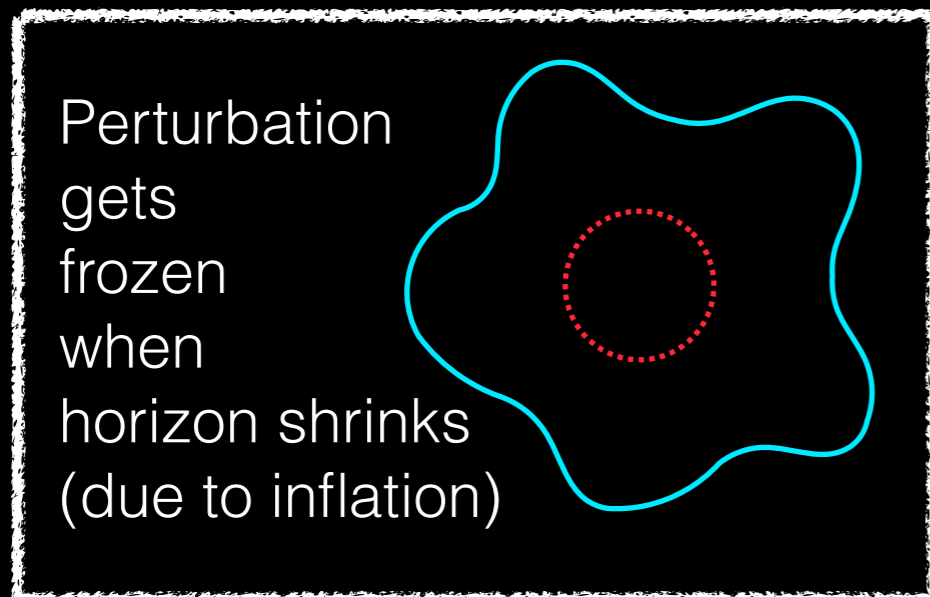
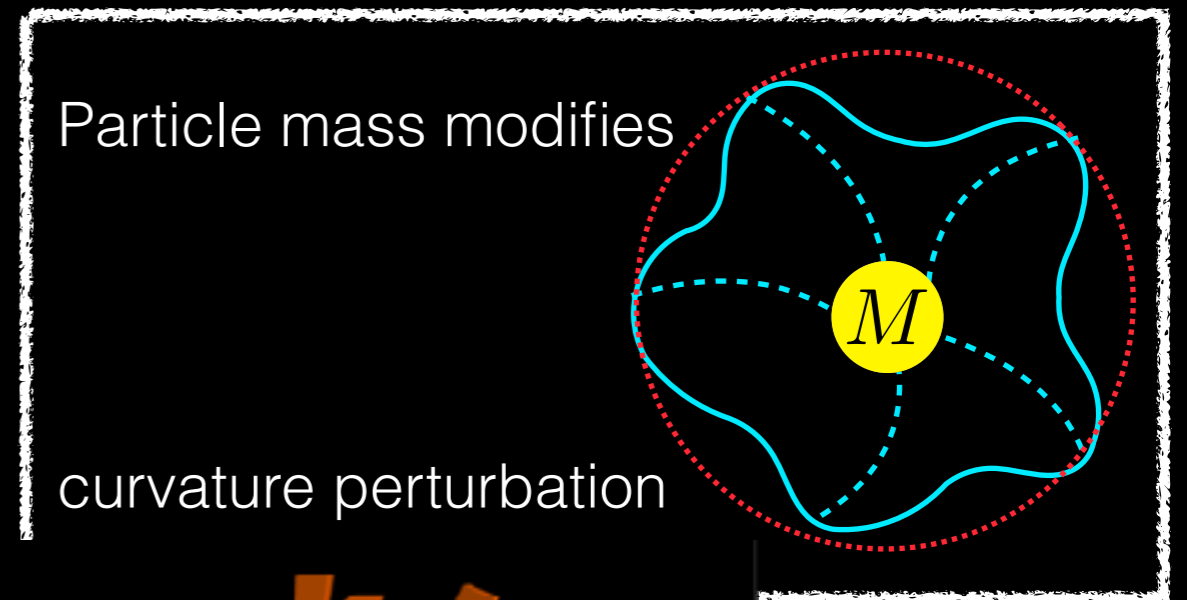
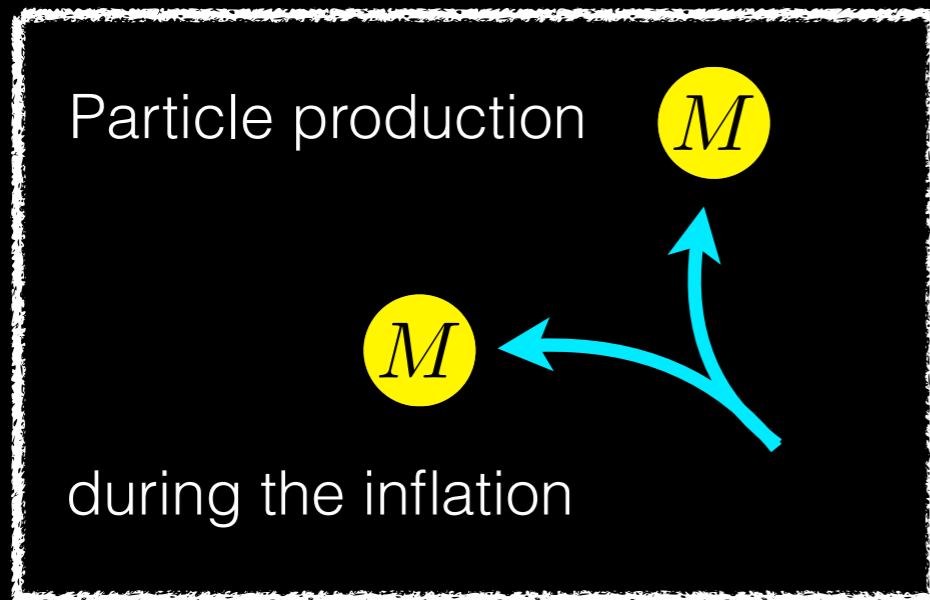
$$N_{\sigma \text{ pairs}} \approx 30$$

# Why pairs? Separation?

- Particles are produced at least in pairs due to **momentum conservation**
- Particles tend to be produced with low momentum. **Separation** given by  $k^{-1}$  is comparable to the horizon size  $|\eta_*|$
- We will model the separation as a **random uniform distribution** between 0 and  $|\eta_*|$

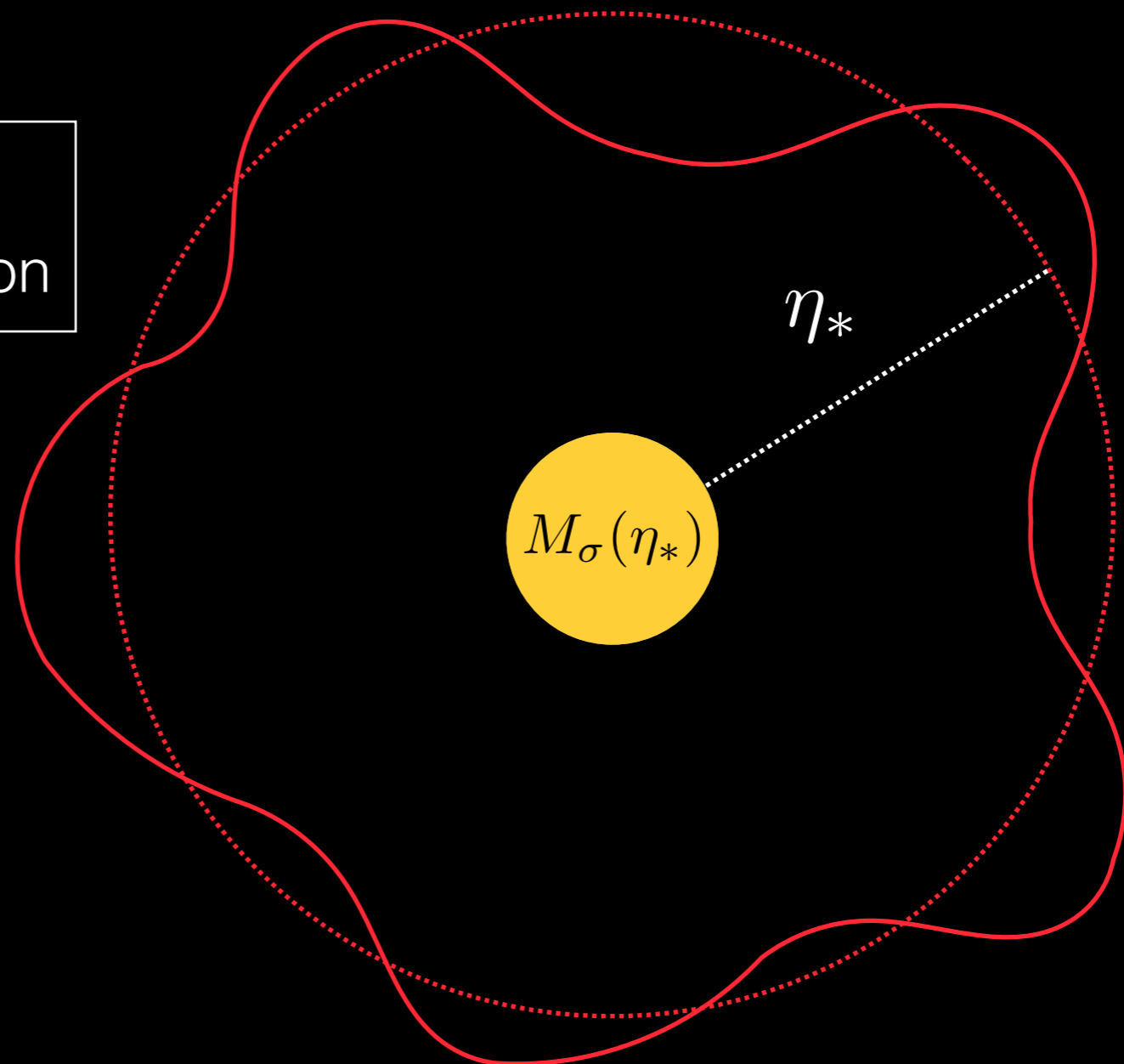


# Step II: mass modifies curvature perturbation



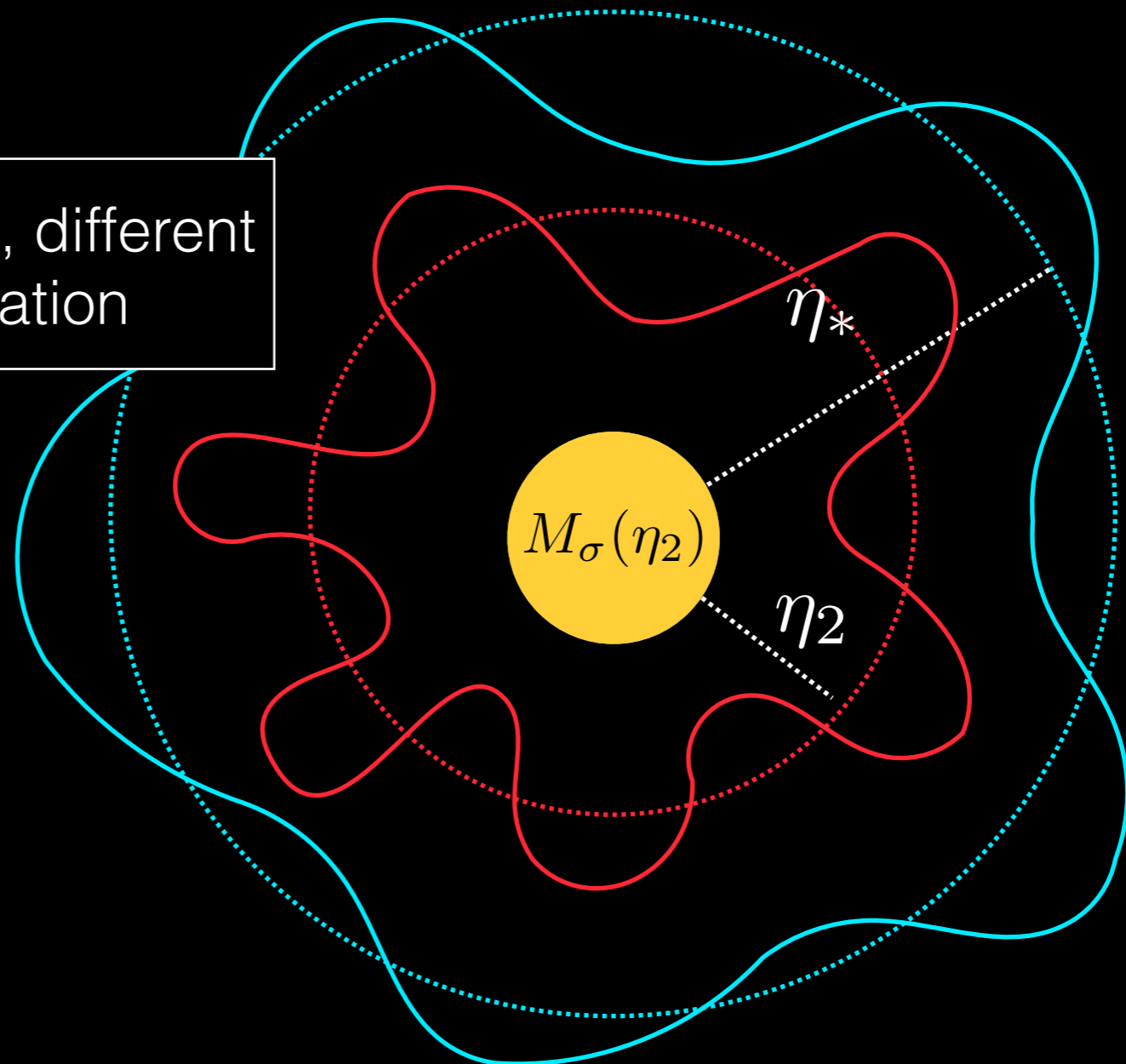
particle mass modifies **curvature perturbation** in the horizon

horizon size  $\sim |\eta_*|$   
at particle production



Once perturbation in the old horizon is frozen, **NEW** particle mass  
Modifies the perturbation in the **NEW** horizon

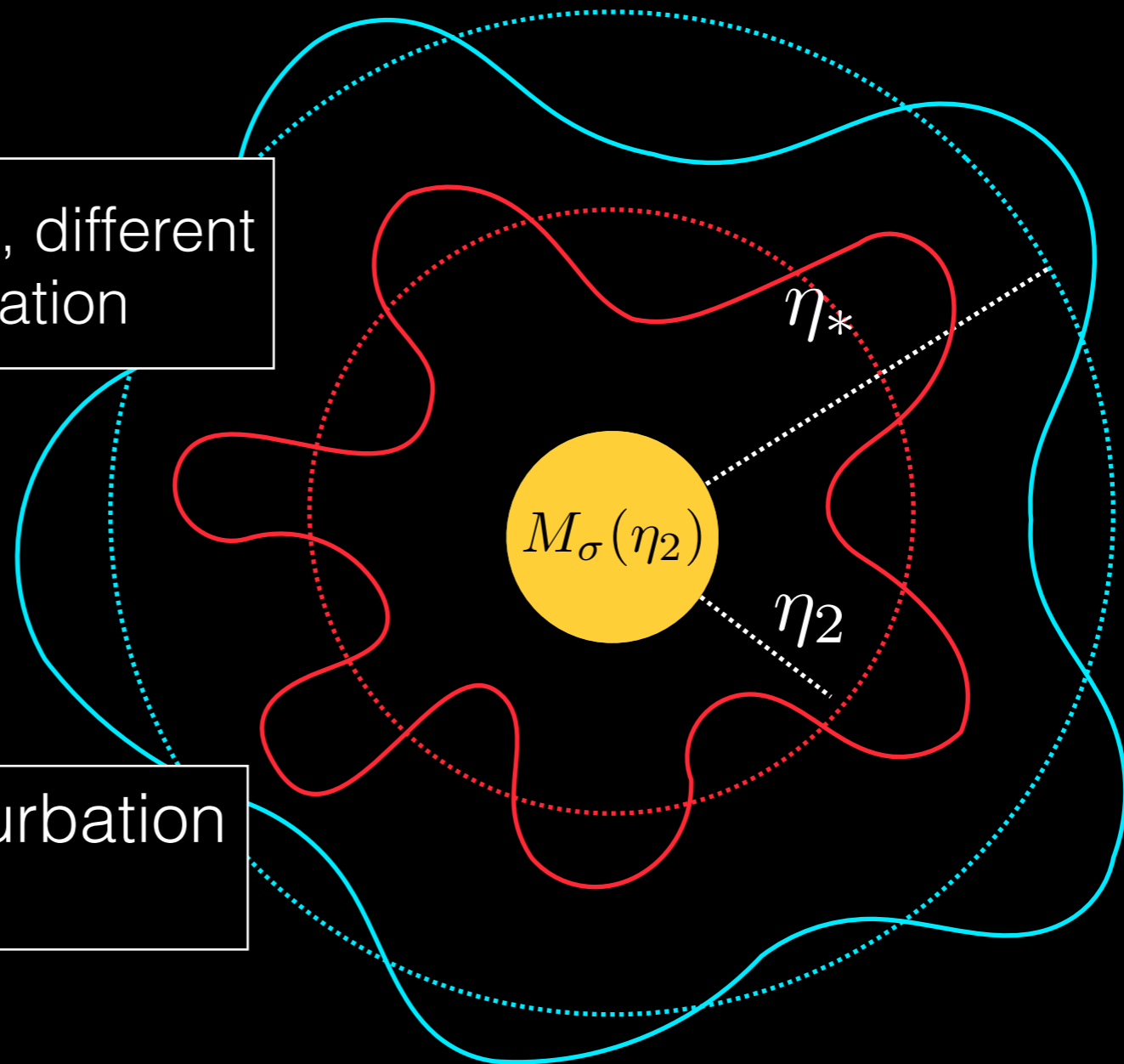
new horizon, different  
perturbation



Once perturbation in the old horizon is frozen, **NEW** particle mass  
Modifies the perturbation in the **NEW** horizon

new horizon, different  
perturbation

**radius-dependent** perturbation  
with  $r < |\eta_*|$



# Curvature perturbation in position space

The resulting curvature profile in  $r \leq |\eta_*|$  from the spot center,

Adiabatic fluctuation  $\langle \zeta_{ad} \rangle = \sqrt{A_s} \sim 10^{-5}$

$$\langle \zeta_\sigma \rangle = \left[ \frac{g}{2} \log \left( \frac{|\eta_*|}{r} \right) \right] \frac{H}{2\pi \sqrt{2\epsilon} M_{pl}} \sim \left[ \frac{g}{2} \log \left( \frac{|\eta_*|}{r} \right) \right] \langle \zeta_{ad} \rangle$$

Spot **size**  $\sim |\eta_*|$  and the coupling  $g$  controls the spot **temperature** over CMB fluctuations



# Curvature perturbation in position space

The resulting curvature profile in  $r \leq |\eta_*|$  from the spot center,

Adiabatic fluctuation  $\langle \zeta_{ad} \rangle = \sqrt{A_s} \sim 10^{-5}$

$$\langle \zeta_\sigma \rangle = \left[ \frac{g}{2} \log \left( \frac{|\eta_*|}{r} \right) \right] \frac{H}{2\pi\sqrt{2\epsilon}M_{pl}} \sim \left[ \frac{g}{2} \log \left( \frac{|\eta_*|}{r} \right) \right] \langle \zeta_{ad} \rangle$$

Spot **size**  $\sim |\eta_*|$  and the coupling  $g$  controls the spot **temperature** over CMB fluctuations

$$\phi - \phi_* = \dot{\phi}(t - t_*) = -\frac{\dot{\phi}}{H_*} \log \left( \frac{\eta}{\eta_*} \right)$$

from the exponential growth during inflation  
 $e^{H_*(t-t_*)} = a/a_* \approx \eta_*/\eta$

# Curvature perturbation in position space

The resulting curvature profile in  $r \leq |\eta_*|$  from the spot center,

Adiabatic fluctuation  $\langle \zeta_{ad} \rangle = \sqrt{A_s} \sim 10^{-5}$

$$\langle \zeta_\sigma \rangle = \left[ \frac{g}{2} \log \left( \frac{|\eta_*|}{r} \right) \right] \frac{H}{2\pi\sqrt{2\epsilon}M_{pl}} \sim \left[ \frac{g}{2} \log \left( \frac{|\eta_*|}{r} \right) \right] \langle \zeta_{ad} \rangle$$

Therefore, the signal profile described below is quite universal!

# Hot or Cold spots?

Perturbation enters in the radiation-dominant & matter-dominant era has temperature fluctuation

$$\left. \frac{\delta T}{T} \right|_{\text{CMB, RD}} = -\frac{1}{3} \langle \zeta_\sigma \rangle \quad \left. \frac{\delta T}{T} \right|_{\text{CMB, MD}} = -\frac{1}{5} \langle \zeta_\sigma \rangle$$

The minus sign comes from the gravity potential (Sachs-Wolfe), makes pairwise spots **COLD** before entering the horizon

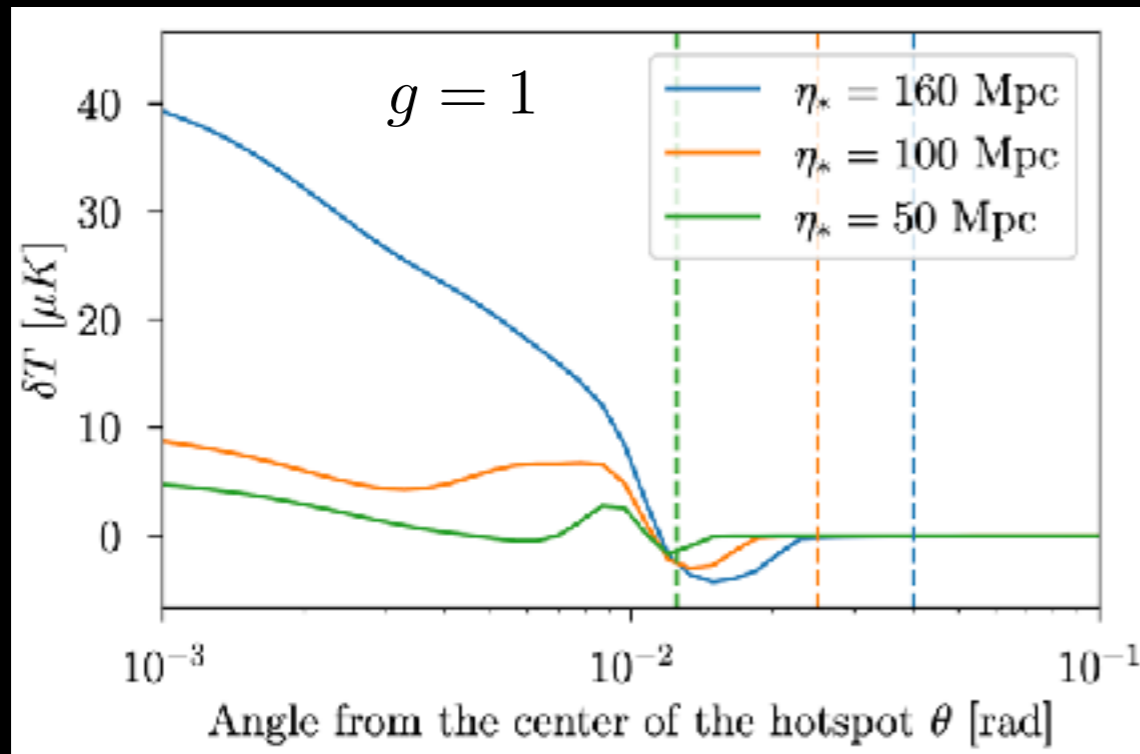
However, we find that the **baryon acoustic oscillation** (sub-horizon phys) converts the signal into **HOT** spots and further changes the fluctuation

$$\theta(\vec{x}_0, \hat{n}, \eta_0) = \frac{4\pi}{(2\pi)^3} \int_0^\infty \frac{dk}{k} \sum_l j_l(k\eta_0 - k\eta_{\text{rec}}) (2l+1) \mathcal{P}_l(\hat{n} \cdot \hat{n}_{\text{HS}}) (f_{\text{SW}}(k) + f_{\text{ISW}}(k)) f(k\eta_*)$$

$$f_{\text{SW}}(k) = T_{\text{SW}}(k) j_l(k\eta_0 - k\eta_{\text{rec}})$$

# Include the effect of “sub-horizon” physics

from baryon acoustic oscillations (the transfer functions)

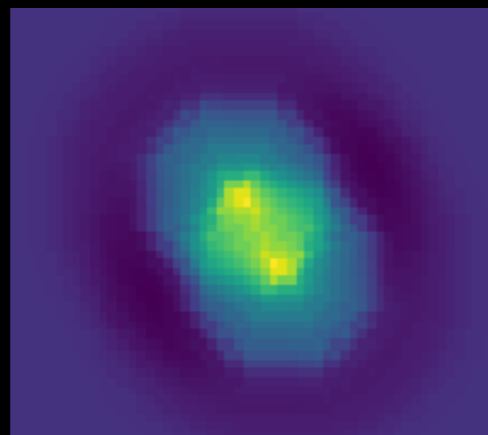


$\eta_*$

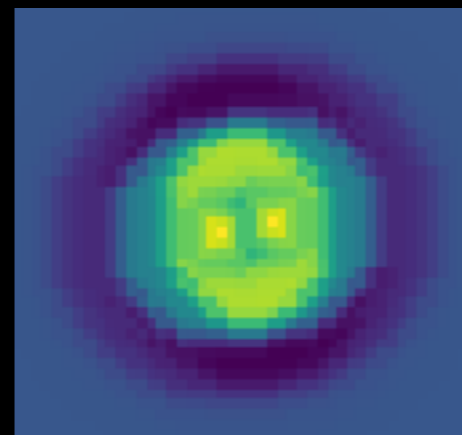
the conformal time & horizon size of particle production

Temperature profile

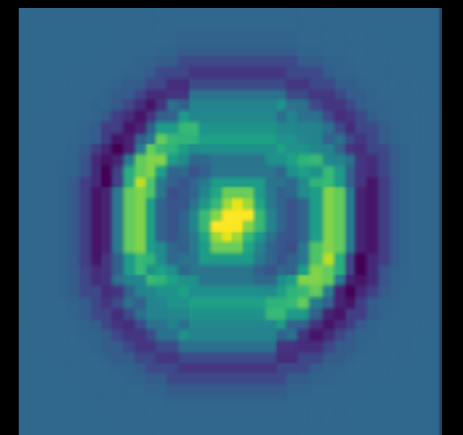
$\eta_* = 160$  Mpc



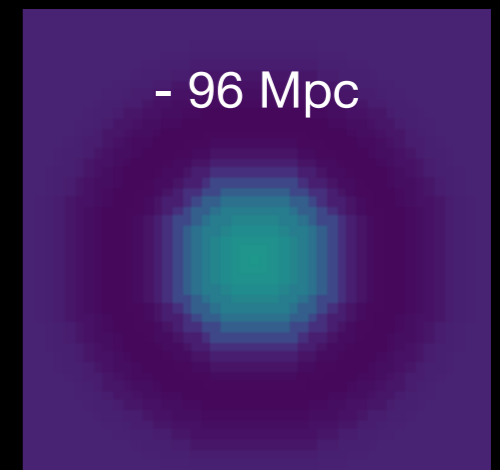
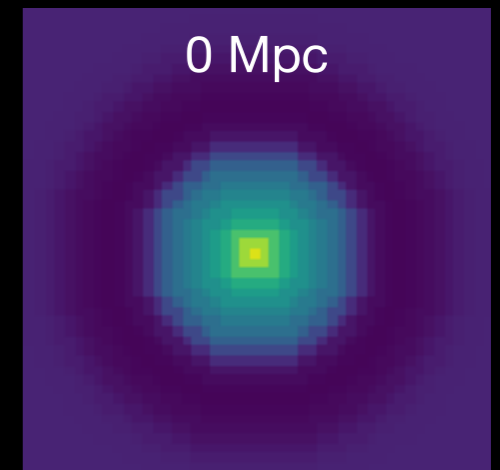
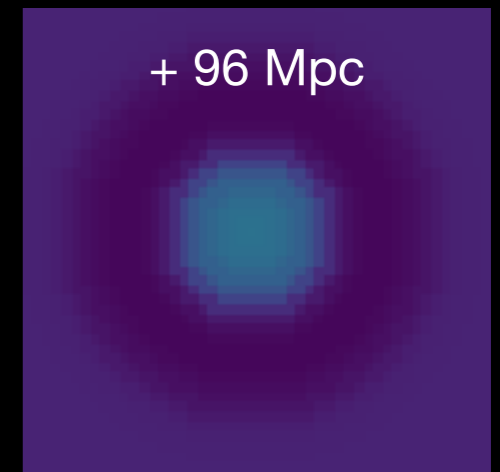
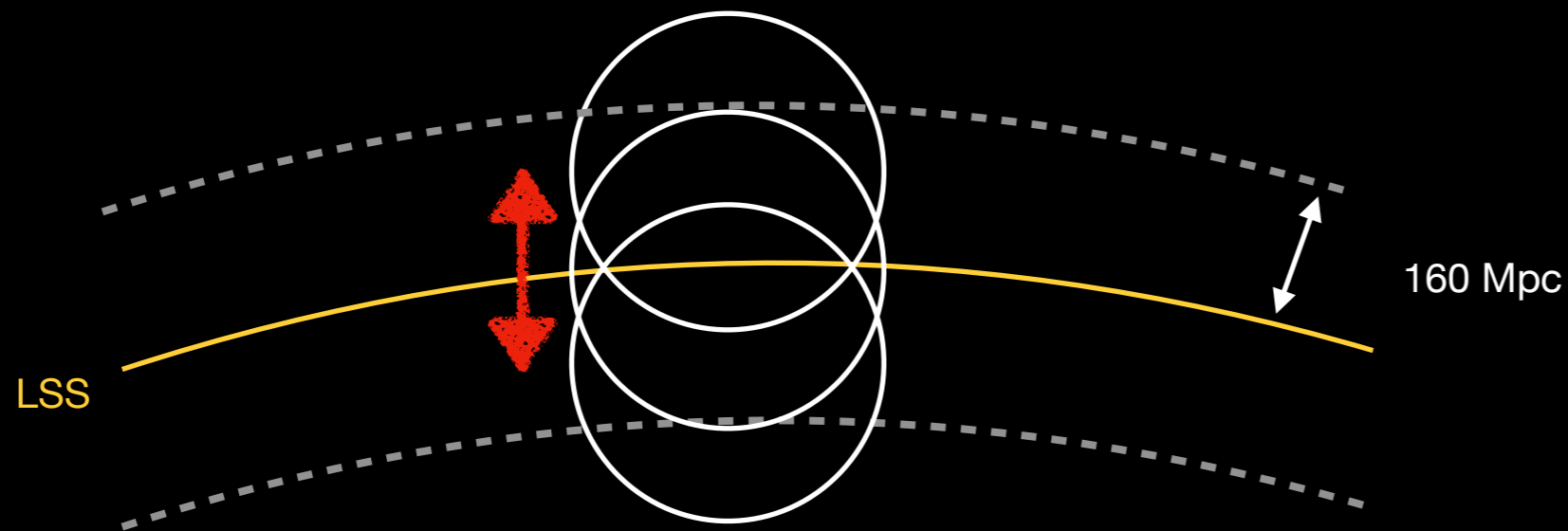
$\eta_* = 100$  Mpc



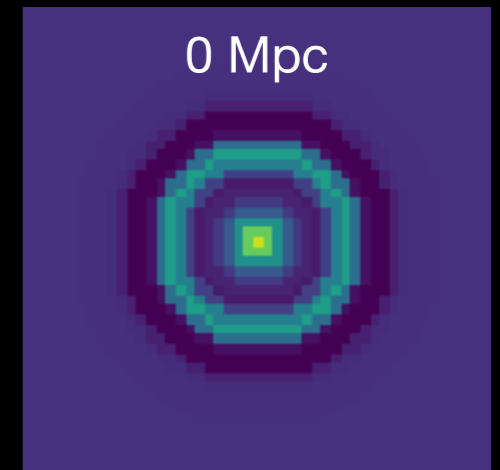
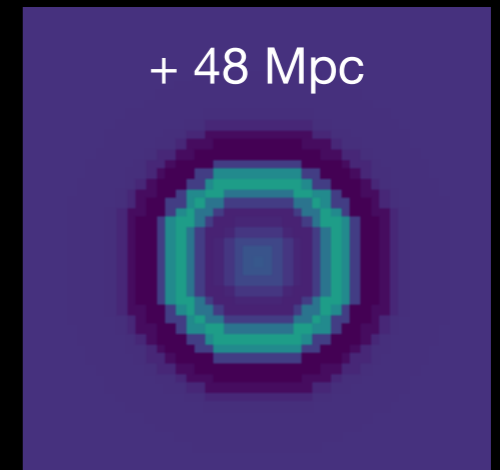
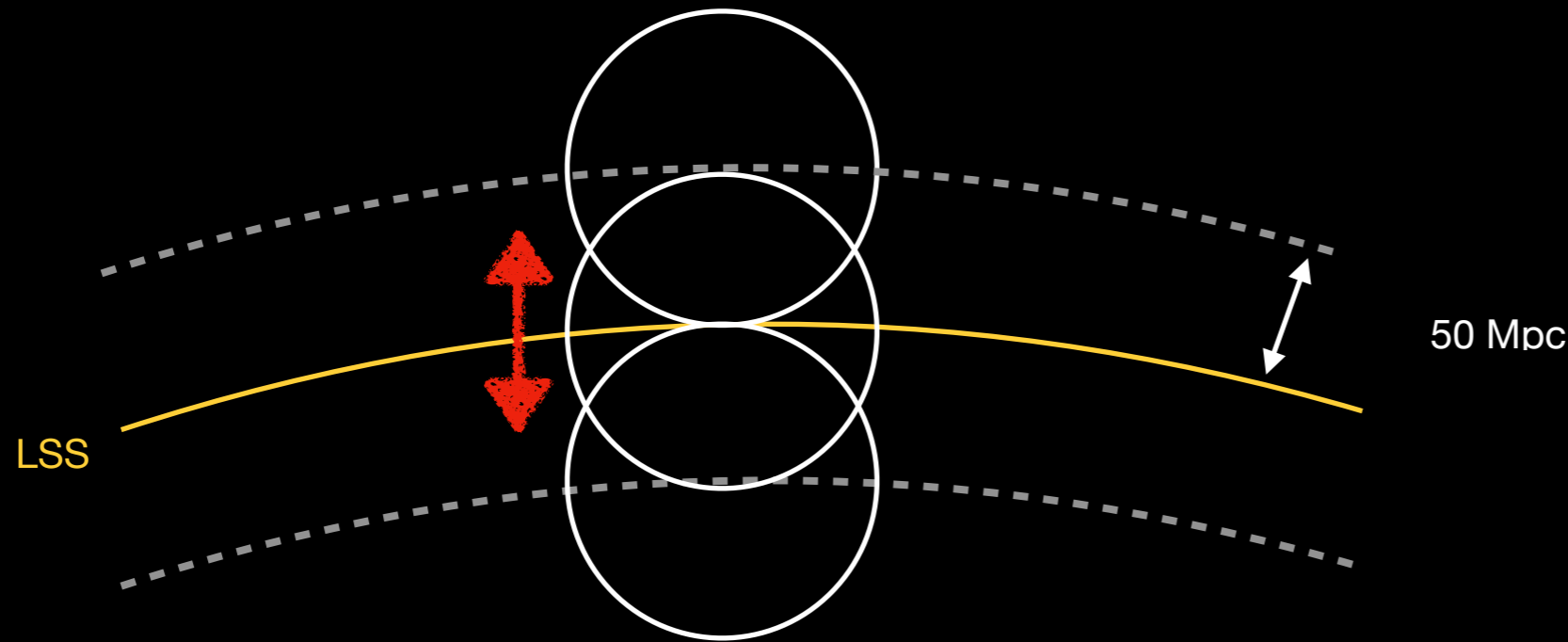
$\eta_* = 50$  Mpc



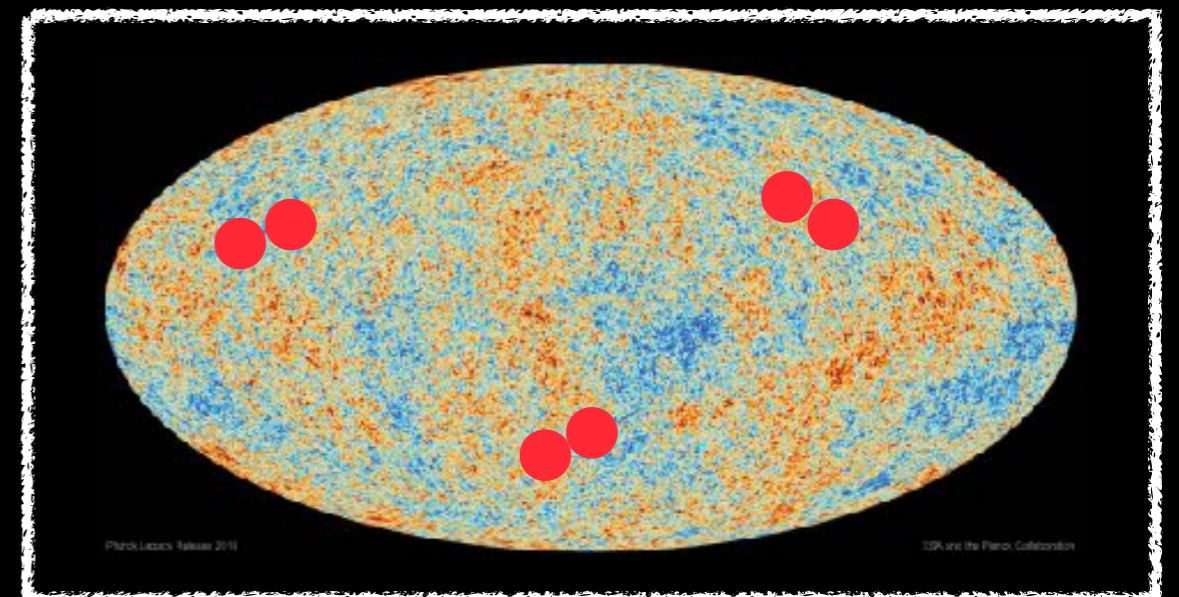
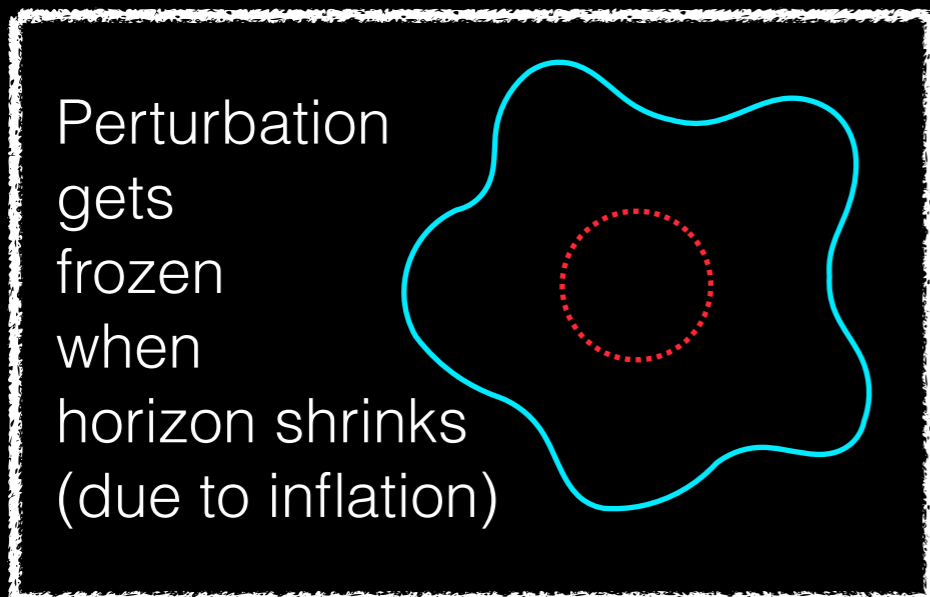
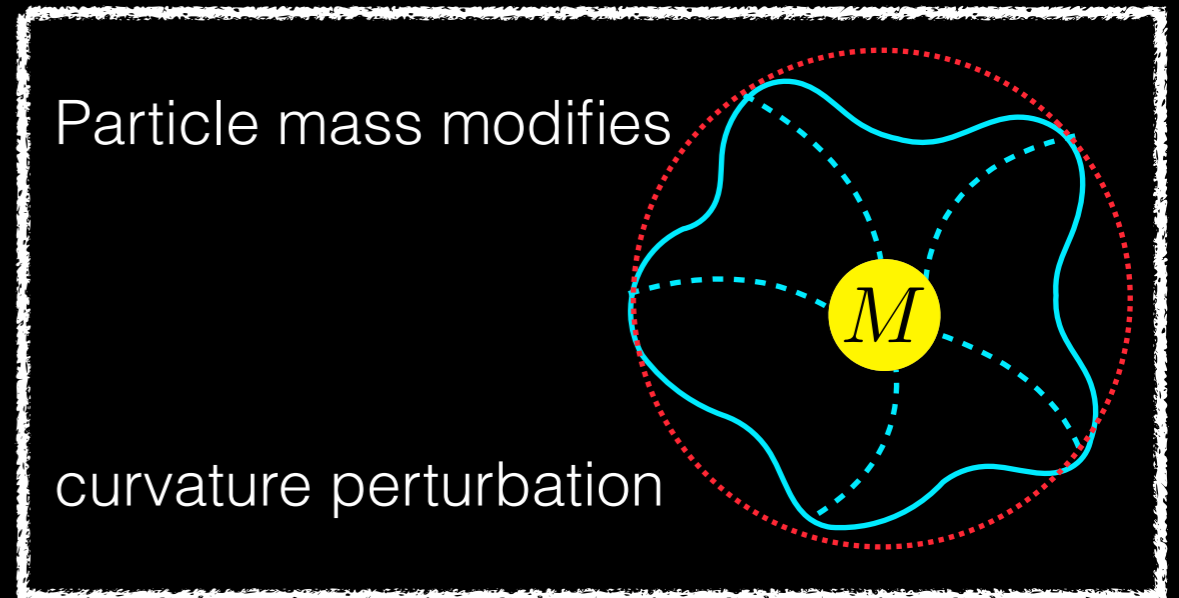
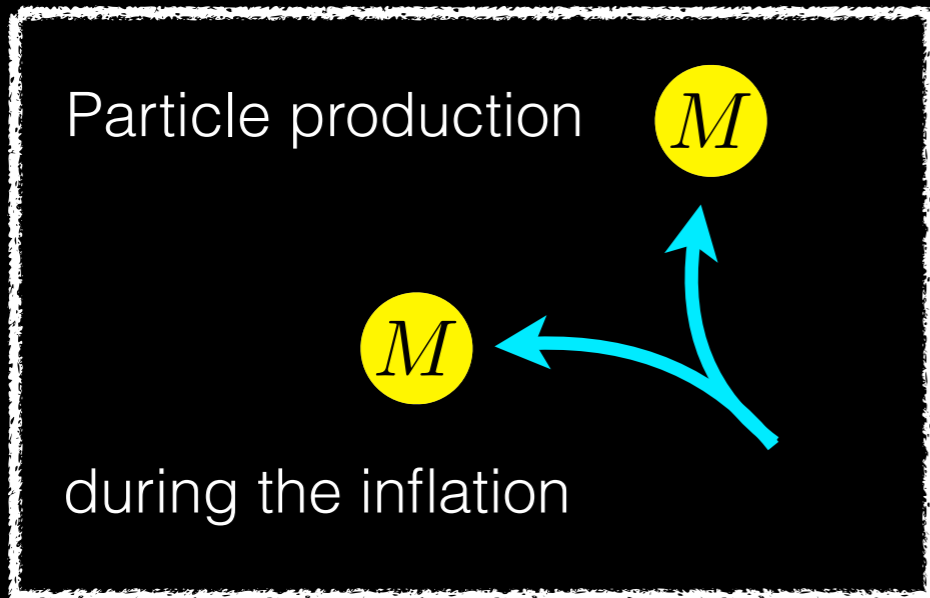
When particles are away from  
the last scattering surface ( $\eta_* = 160$  Mpc)



When particles are away from  
the last scattering surface ( $\eta_* = 50$  Mpc)



# Step III: localized signals on the CMB



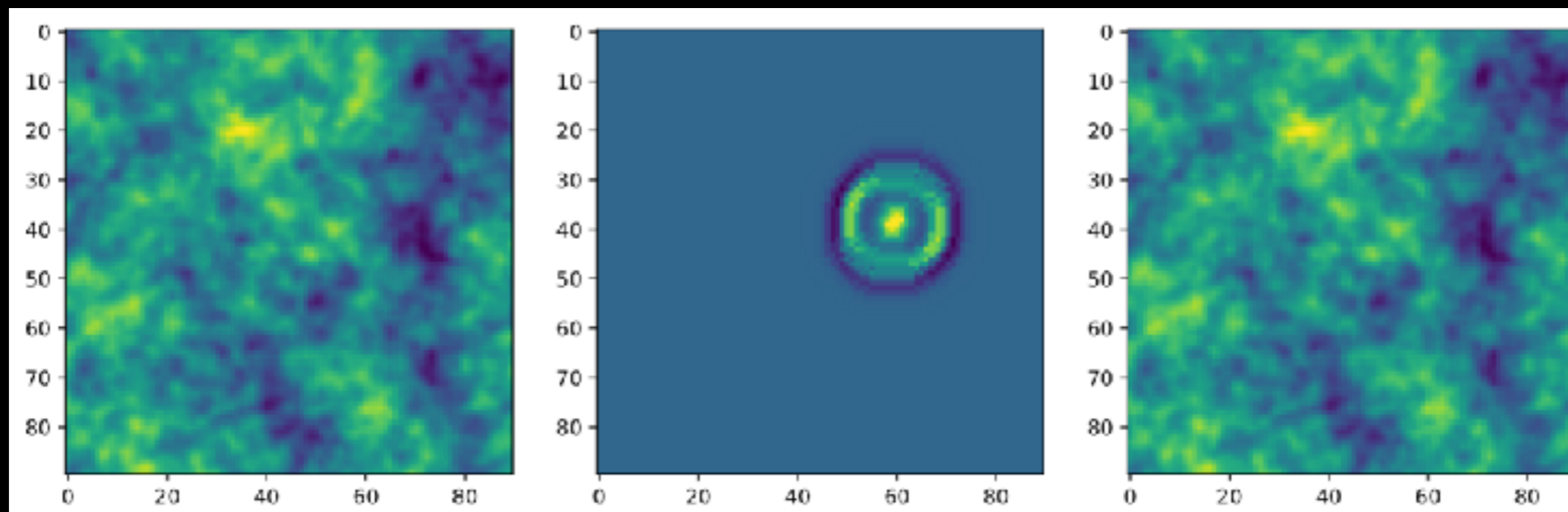
# Simulate pairwise spot signals

- use [QuickLens](#) to generate fake CMB images that follow the temperature fluctuation of the best fitted LCDM model
- for signal events, add pairwise hotspots with a given temperature profile, pixel size, and separation between two spots

simulated CMB

signal

simulated CMB + signal



$$\eta_* = 50 \text{ Mpc}$$

$$g = 4$$



# Identify signal on the CMB map

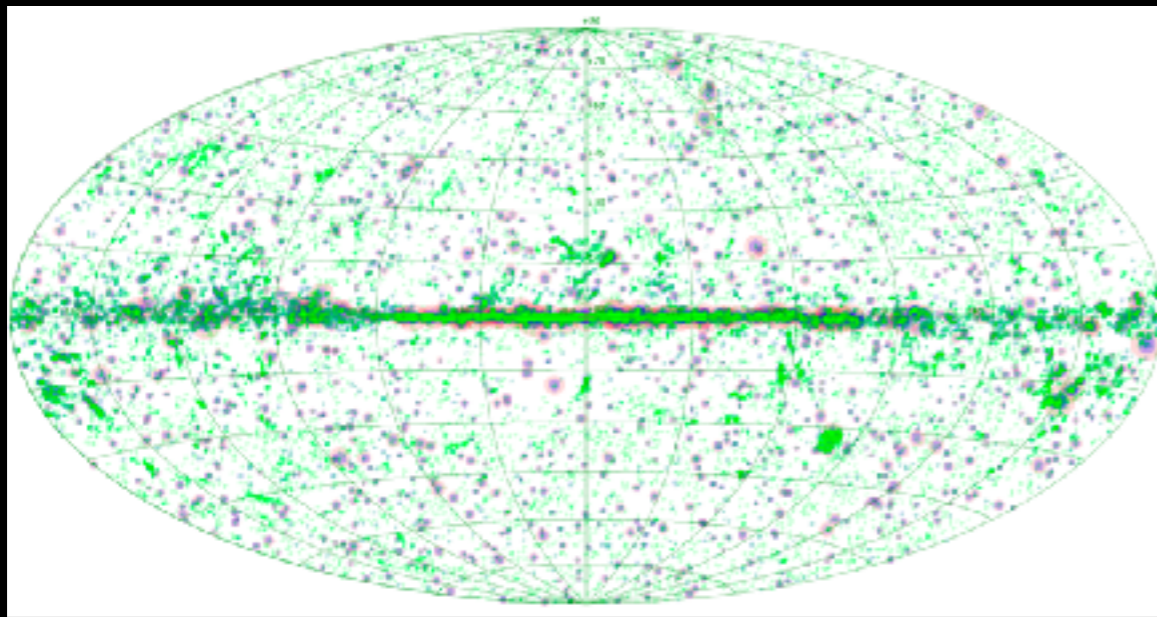
Different types of backgrounds to consider:

- instrumental noise: (not an issue for Planck)
- fore-ground from compact objects (stars, galaxies,...)
- primordial fluctuation background (indistinguishable)

# Identify signal on the CMB map

Different types of backgrounds to consider:

- instrumental noise: (not an issue for Planck)
- fore-ground from compact objects (stars, galaxies,...)
- primordial fluctuation background (indistinguishable)



Can veto the background by correlating Planck's maps with 9 frequency bands

Easier to identify compact objects  $> \sim 10$  Mpc  
A common lore is that "WMAP is foreground-free"

Planck 2013 results. XXVIII

**Fig. 1.** Sky distribution of the PCCS sources at three different channels: 30 GHz (pink circles); 143 GHz (magenta circles); and 857 GHz (green circles). The dimension of the circles is related to the brightness of the sources and the beam size of each channel. The figure is a full-sky Aitoff projection with the Galactic equator horizontal; longitude increases to the left with the Galactic centre in the centre of the map.

# Identify signal on the CMB map

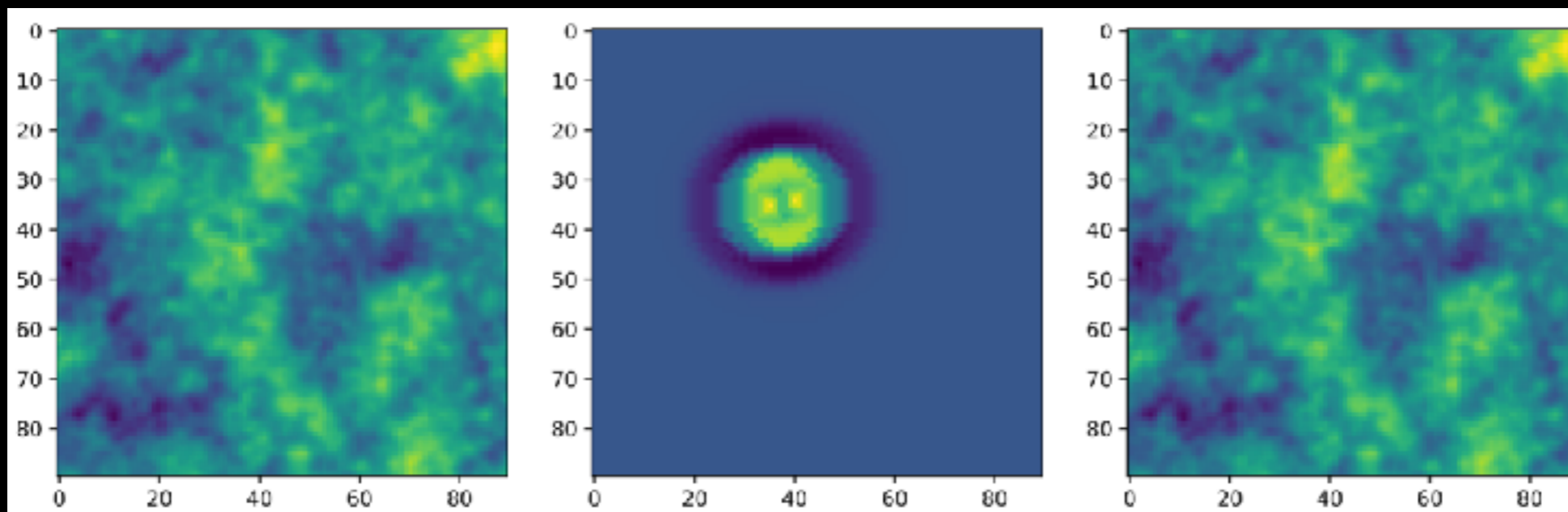
Different types of backgrounds to consider:

- instrumental noise: (not an issue for Planck)
- fore-ground from compact objects (stars, galaxies,...)
- **primordial fluctuation background** (indistinguishable)

simulated CMB

signal

simulated CMB + signal



$$\eta_* = 50 \text{ Mpc}$$

$$g = 4$$

# Convolutional Neural Network (CNN)

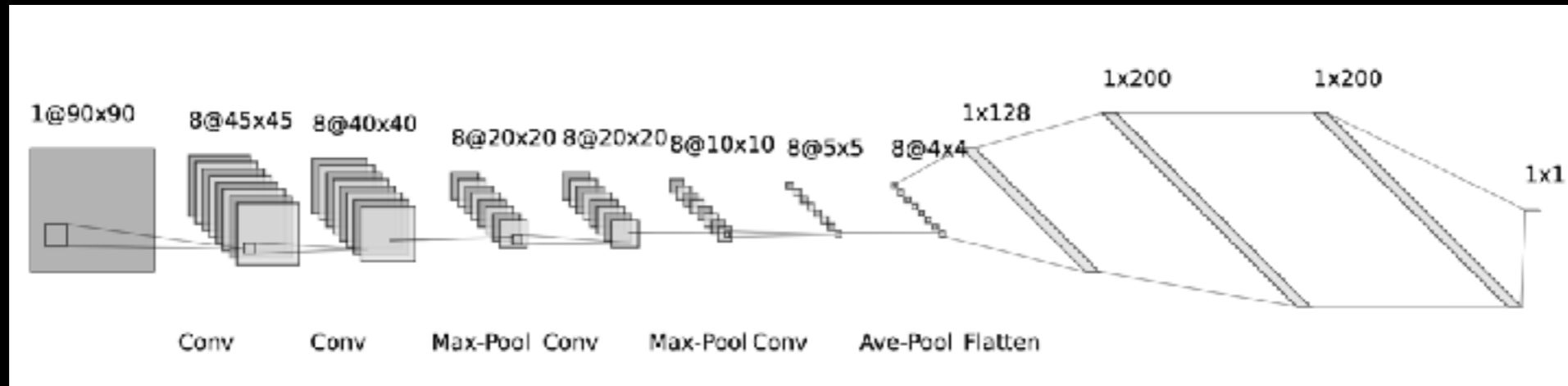
Instead of matched filter, we use the CNN to dig out the signal from background

CNN analysis works better for signals with **non-spherical** and **varying** profiles

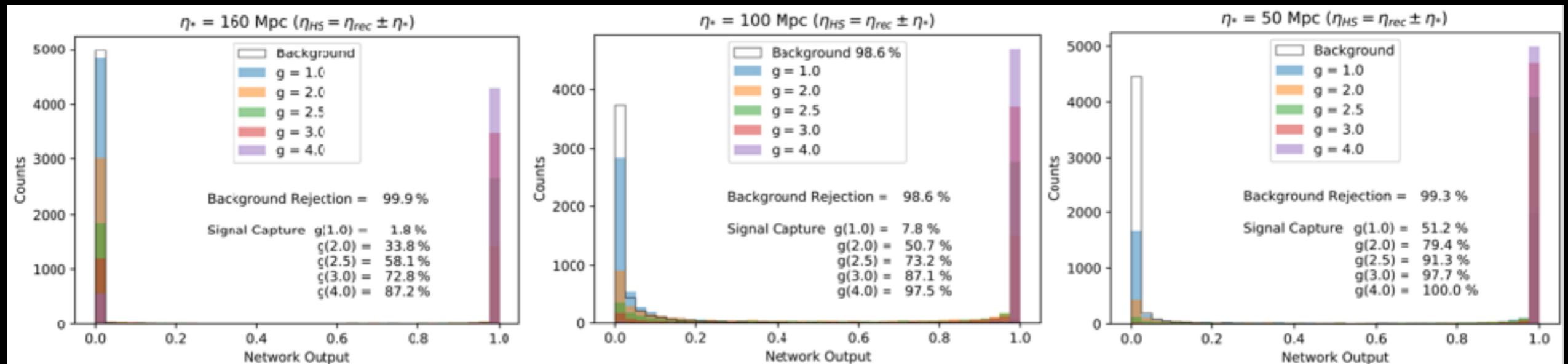
We cross check the result between CNN and MF using signals with fixed profiles, and most of the results are similar

# Convolutional Neural Network (CNN)

## Our CNN structure

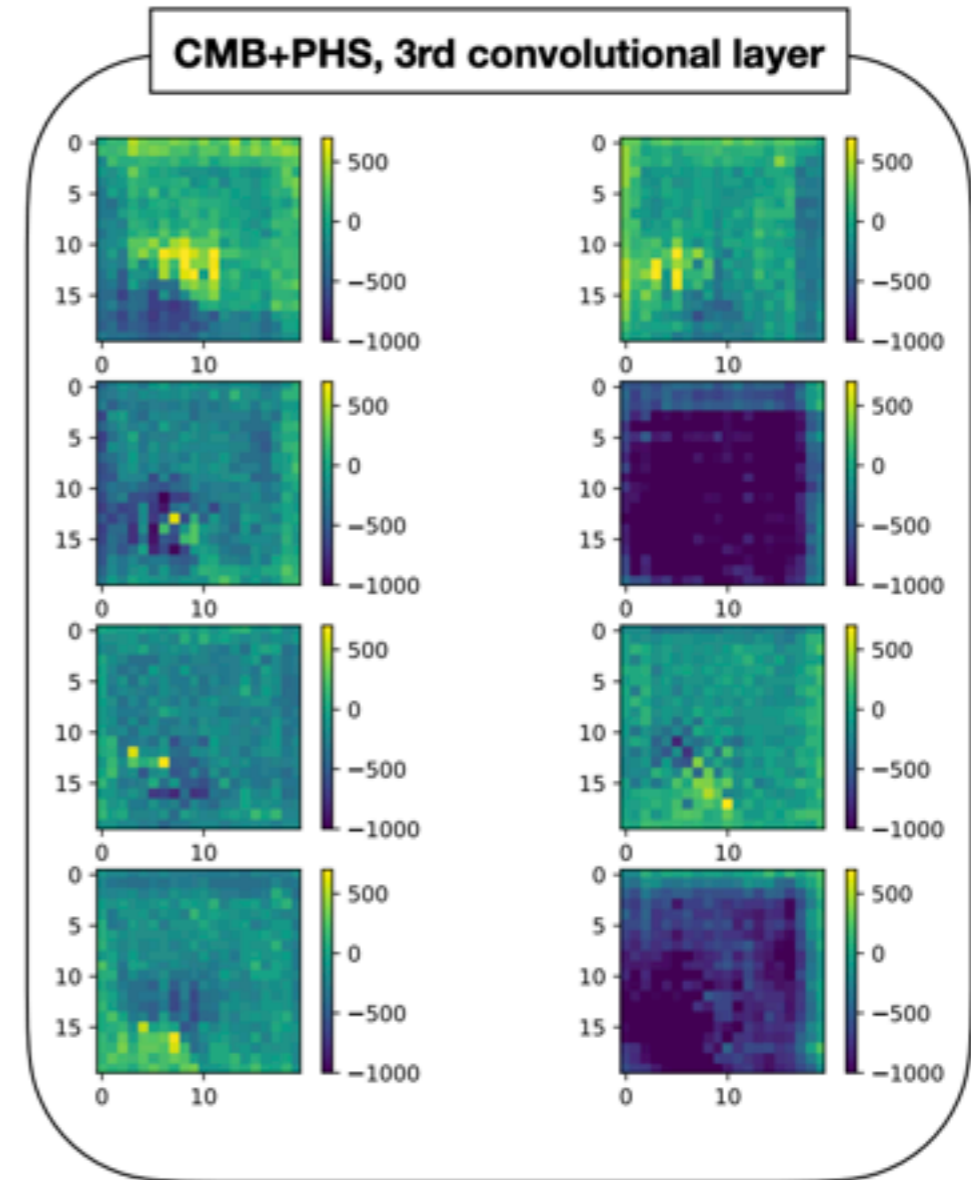
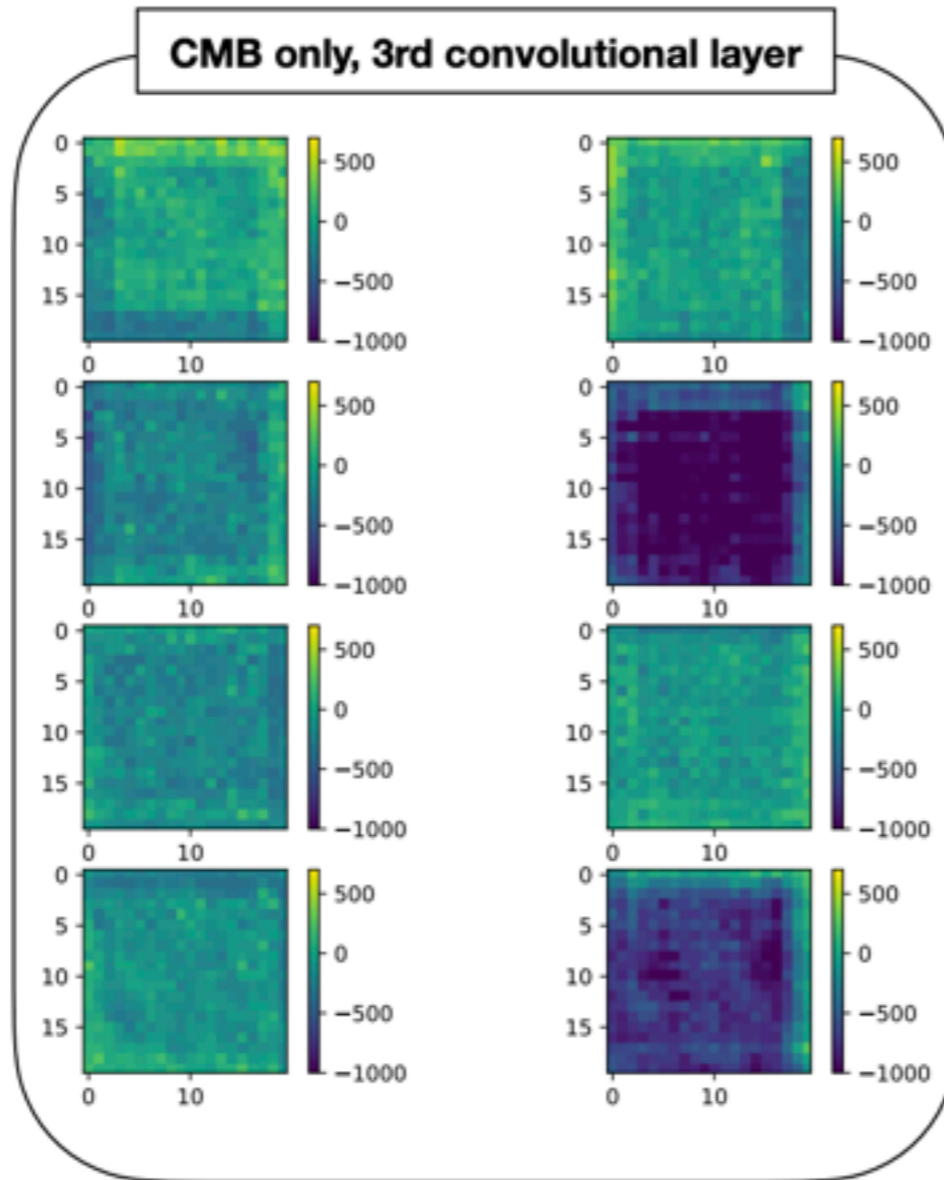
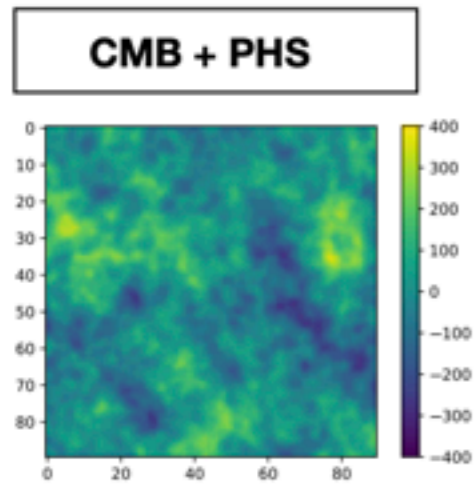
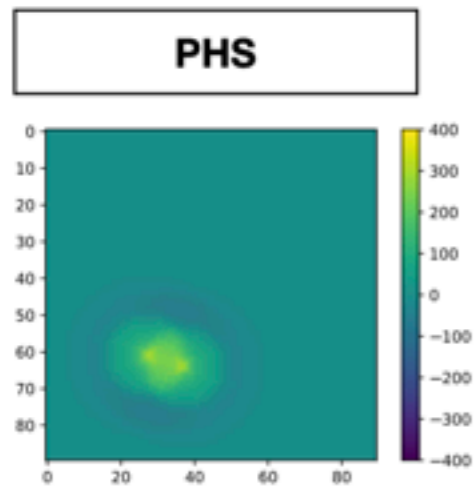


Train the CNN with 160k smaller size images (w/ & w/o signal injection)  
Network outputs the probability of having a signal in the image



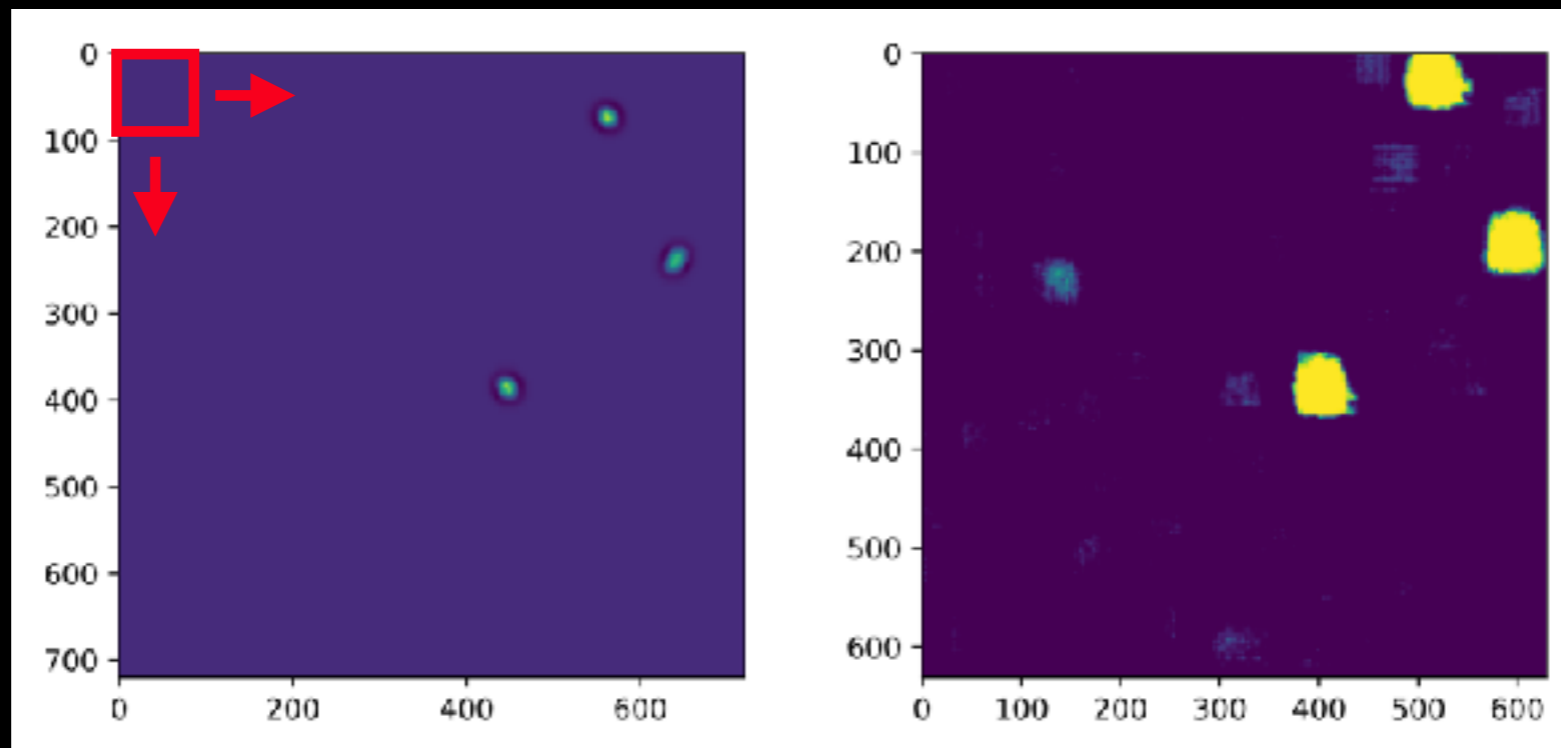
# Results from the 3rd convolutional layer

$\eta_* = 160 \text{ Mpc}, g = 4$



# Convolutional Neural Network (CNN)

Apply the same network to a larger image ( $\sim 1/25$  of the sky), sliding the search box, convert the map into a “probability map”



With “clustering” and vetoing clusters with small pixel numbers, we calculate the signal capture rate & false positive rate

# Result: $2\sigma$ exclusion bound

with sky fraction = 60% (similar to the Planck analysis)

Number of PHS	$\eta = 50$	$\eta = 100$	$\eta = 160$
$g = 1$	8	840	1162
$g = 2$	5	20	17
$g = 3$	4	9	8

$M_0/H_I$	$\eta = 50$	$\eta = 100$	$\eta = 160$
$g = 1$	145	120	114
$g = 2$	213	199	194
$g = 3$	266	253	247

$M_0/(g\dot{\phi}_0)^{1/2}$	$\eta = 50$	$\eta = 100$	$\eta = 160$
$g = 1$	2.5	2.0	2.0
$g = 2$	2.6	2.4	2.4
$g = 3$	2.6	2.5	2.4

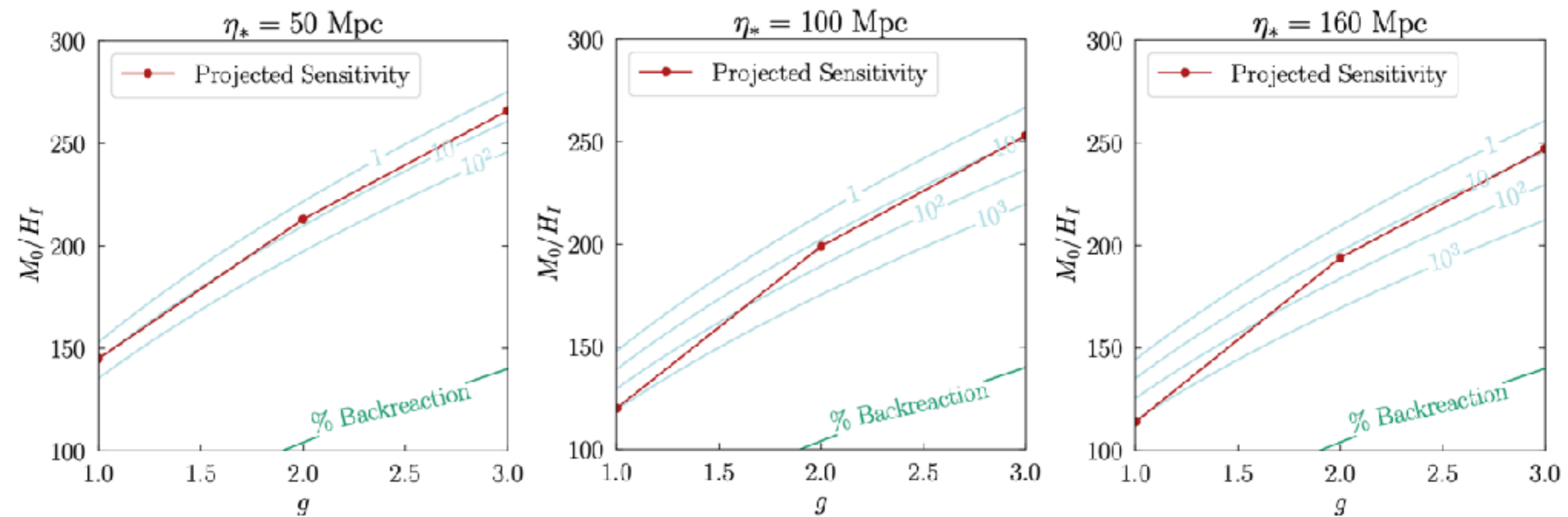
**Table 2.** *Upper:*  $2\sigma$  upper bound on the number of PHS in the whole CMB sky with both hotspot centers located within  $\eta_{\text{rec}} \pm \eta_*$  window around the last scattering surface. In the calculation we assume sky fraction  $f_{\text{sky}} = 60\%$ . *Lower left:* lower bounds on the bare mass of the heavy scalar field in units of the Hubble scale during the inflation. *Lower right:* lower bounds on the bare mass in units of the rate of the mass,  $(g\dot{\phi}_0)^{1/2}$ , owing to the inflaton coupling.

$$N_{\sigma \text{ pairs}} = \frac{1}{2\pi^2} \left( \frac{g\dot{\phi}_0}{H_I^2} \right)^{3/2} e^{-\frac{\pi(M_0^2 - 2H_I^2)}{g|\dot{\phi}|}} \left( \frac{\eta_0}{\eta_*} \right)^3 \frac{\Delta\eta}{\eta_0}$$



# Result: $2\sigma$ exclusion bound

with sky fraction = 60% (similar to the Planck analysis)



The CNN analysis can (in principle) set mass bounds close to the optimal limit allowed by the CMB search

# Back-reaction constraints

Need to make sure the scalar field

does not affect inflaton's slow-roll motion  $3H_*\dot{\phi} \approx -\frac{\partial V_\phi}{\partial\phi}$

Since  $\frac{\partial V}{\partial\phi} = \frac{\partial V_\phi}{\partial\phi} + g(g\phi - M)\sigma^2$

this requires  $g(g\phi - M)\sigma^2 \sim gM_\sigma\sigma^2 \sim gn_\sigma \ll H_*\dot{\phi}$

(similar bound for not depleting inflaton's energy  $M_\sigma n_\sigma \ll \dot{\phi}$ )

**Radiative correction** => assume a UV completion (e.g. SUSY)  
takes care of that (see e.g., Flauger et al. (2016) )

# Result: $5\sigma$ discovery reach

with sky fraction = 60% (similar to the Planck analysis)

Number of PHS	$\eta = 50$	$\eta = 100$	$\eta = 160$
$g = 1$	16	2047	2757
$g = 2$	10	48	40
$g = 3$	9	21	19

$M_0/H_I$	$\eta = 50$	$\eta = 100$	$\eta = 160$
$g = 1$	143	116	110
$g = 2$	210	194	189
$g = 3$	262	247	241

$M_0/(g\dot{\phi})^{1/2}$	$\eta = 50$	$\eta = 100$	$\eta = 160$
$g = 1$	2.4	2.0	1.9
$g = 2$	2.5	2.3	2.3
$g = 3$	2.6	2.4	2.4

Table 3. Same as Table 2 but for the  $5\sigma$  discovery reach.

$$N_{\sigma \text{ pairs}} = \frac{1}{2\pi^2} \left( \frac{g\dot{\phi}_0}{H_I^2} \right)^{3/2} e^{-\frac{\pi(M_0^2 - 2H_I^2)}{g|\dot{\phi}|}} \left( \frac{\eta_0}{\eta_*} \right)^3 \frac{\Delta\eta}{\eta_0}$$

# Conclusion

Production of heavy particles with **inflaton-dependent** mass generate **pairwise spots** on the CMB map

Signal hotspots have a **well-predicted profile** that only depends on  $(g, \eta_*)$

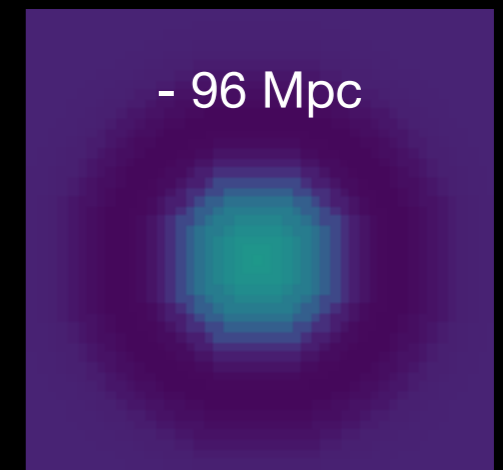
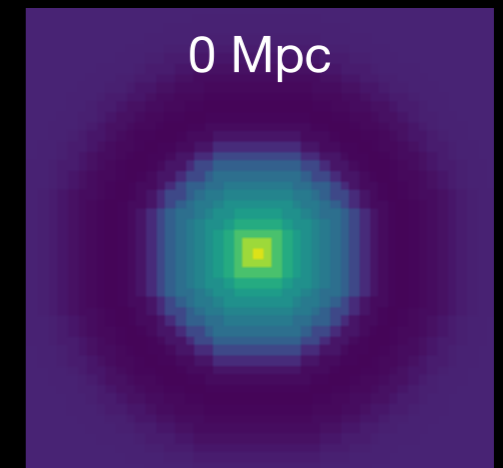
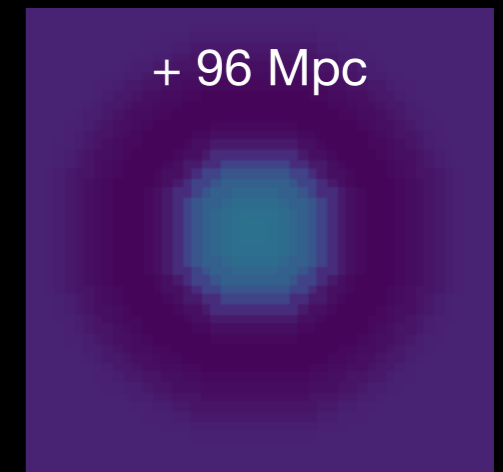
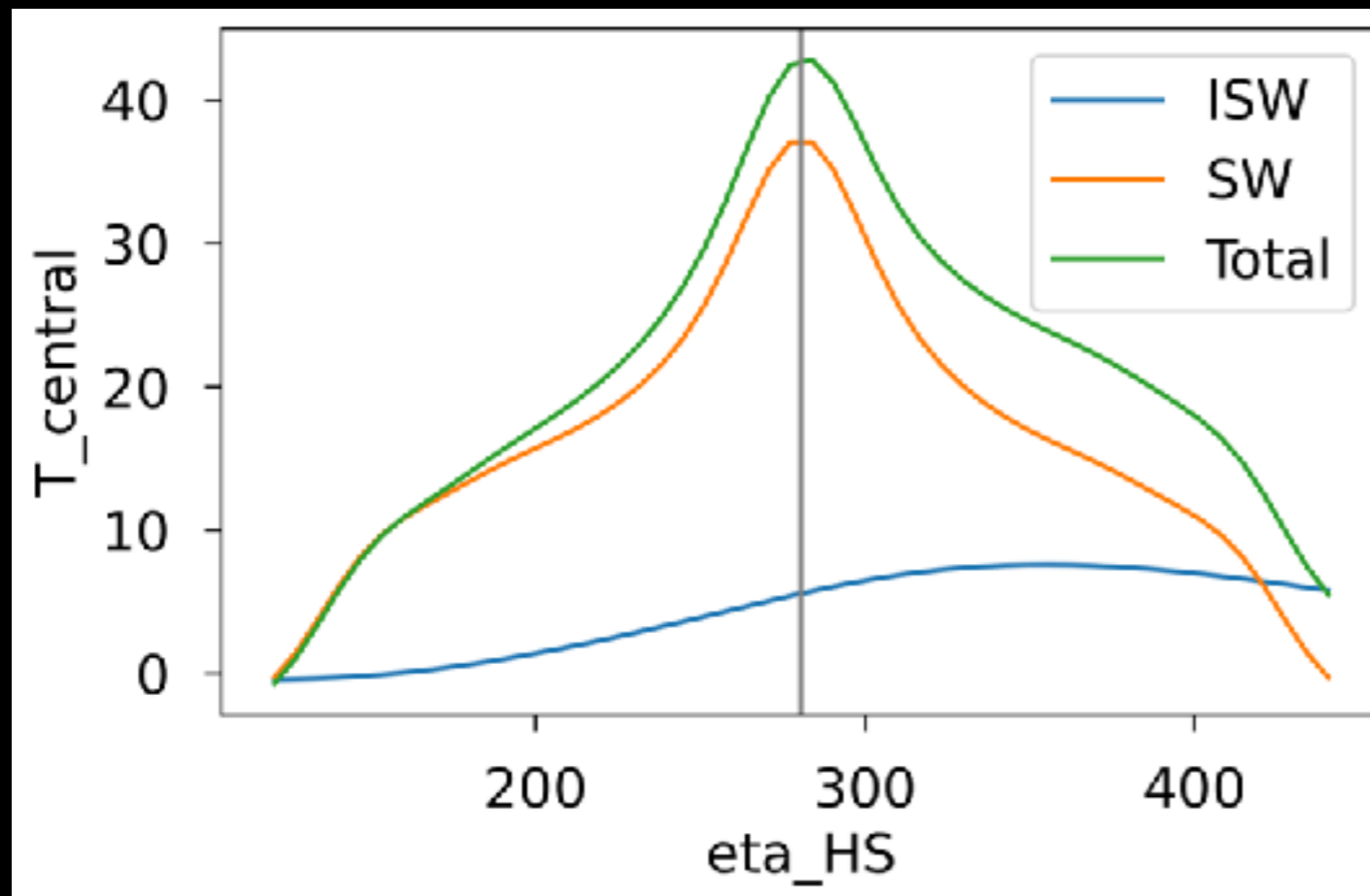
**CNN** can provide a powerful **position space** search of the signal

## **More things to explore:**

- other localized signals for the position space search?
- pairwise clumps in Large Scale Structure? CMB lensing, cosmic shear, etc?
- Including the foreground?

Backup Slides

When particles are away from  
the last scattering surface ( $\eta_* = 160$  Mpc)



	$\omega_b$	$\omega_{\text{cdm}}$	$10^9 A_s$	$n_s$	$\tau_{re}$	Bg rejection	Sig capture
Planck18	0.0224	0.120	2.10	0.966	0.0543	99.8%	74.0%
Case 1		+0.004				99.8%	72.3%
Case 2			+0.07			99.2%	74.1%
Case 3				+0.01		99.6%	69.9%
Case 4	+0.0003					99.8%	73.4%
Case 5					+0.014	99.2%	74.4%
Case 6	+0.0003	-0.004	+0.05	-0.01	-0.014	99.8%	72.4%

**Table 4.** The response of the signal capture and background rejection rates with varying  $\Lambda$ CDM parameters, labeled with the difference to the  $\Lambda$ CDM parameters. The variation of the rates is comparable to the fluctuations in our CNN analysis due to finite sampling and therefore is insignificant. For this test, we used  $g = 2$  and  $\eta_* = 160$  Mpc for the PHS signal.